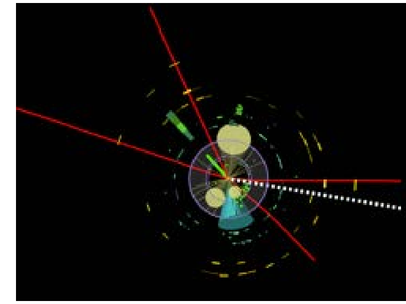

Scalar sector highlights from the **ATLAS** experiment

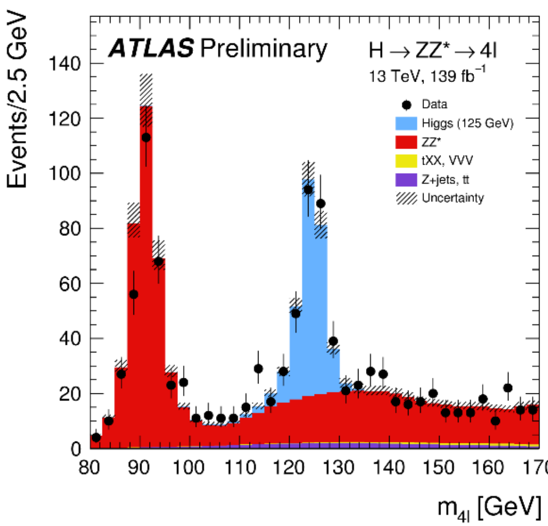

Alan Barr

University of Oxford

*On behalf of the **ATLAS** collaboration*

$$\mathcal{L}_{\mathrm{SM}} = \mathcal{L}_{SM}^{(4)} + \frac{1}{\Lambda}\sum_k C_k^{(5)} Q_k^{(5)} + \frac{1}{\Lambda^2}\sum_k C_k^{(6)} Q_k^{(6)} + \mathcal{O}\left(\frac{1}{\Lambda^3}\right)$$

A much larger dataset

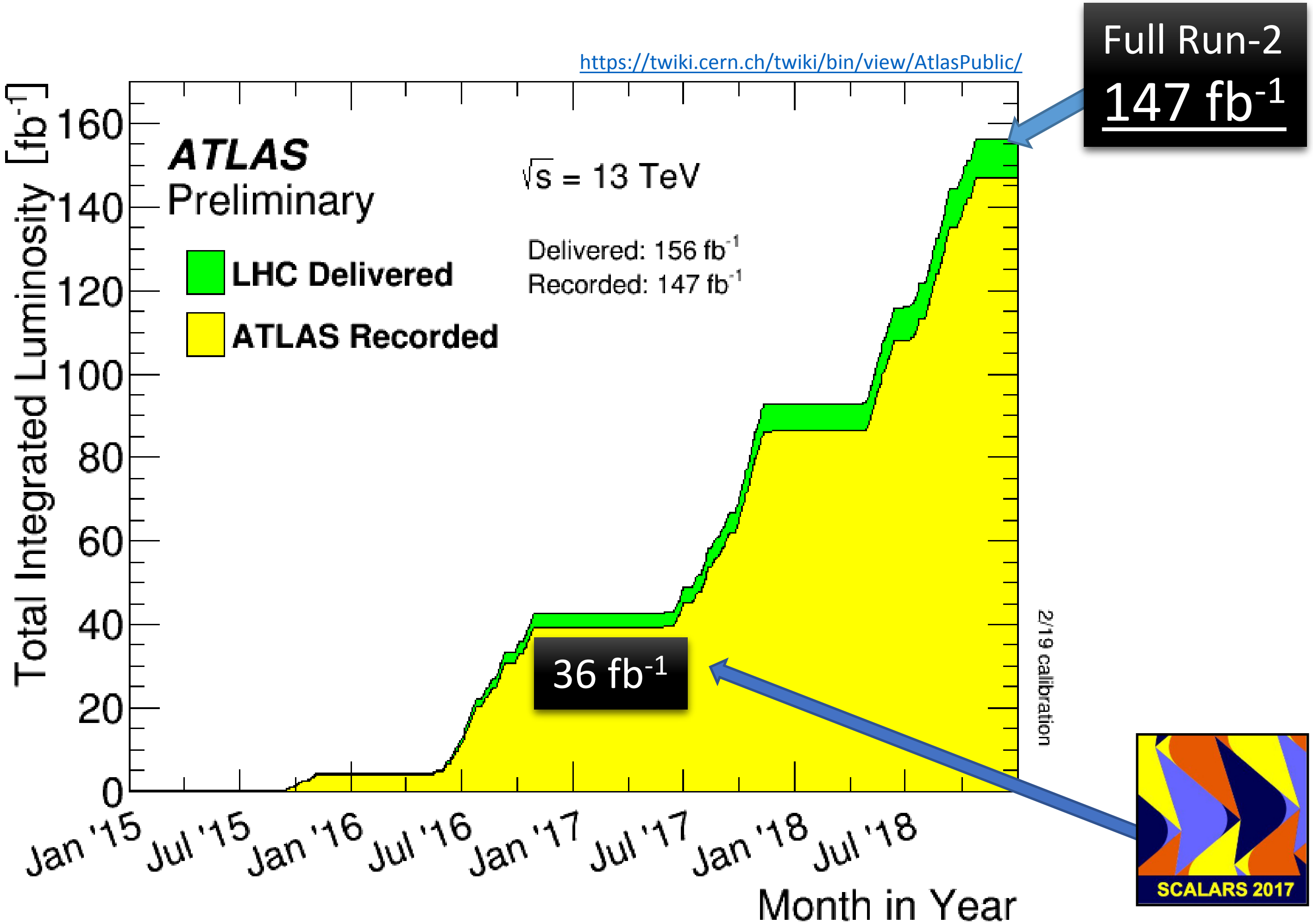

A factory for many things

Particle	Produced in 139 fb^{-1} at $\sqrt{s}$ = 13 TeV	
Higgs boson	7.7 million	
Top quark	275 million	
Z boson	2.8 billion	($\rightarrow \ell\ell$, 290 million)
W boson	12 billion	($\rightarrow \ell\nu$, 3.7 billion)
Bottom quark	$\sim$40 trillion	(significantly reduced by acceptance)

Andreas Hoecker, EPS-HEP-2019

The “discovery” plots…
…but with all that data

ATLAS-CONF-2019-025

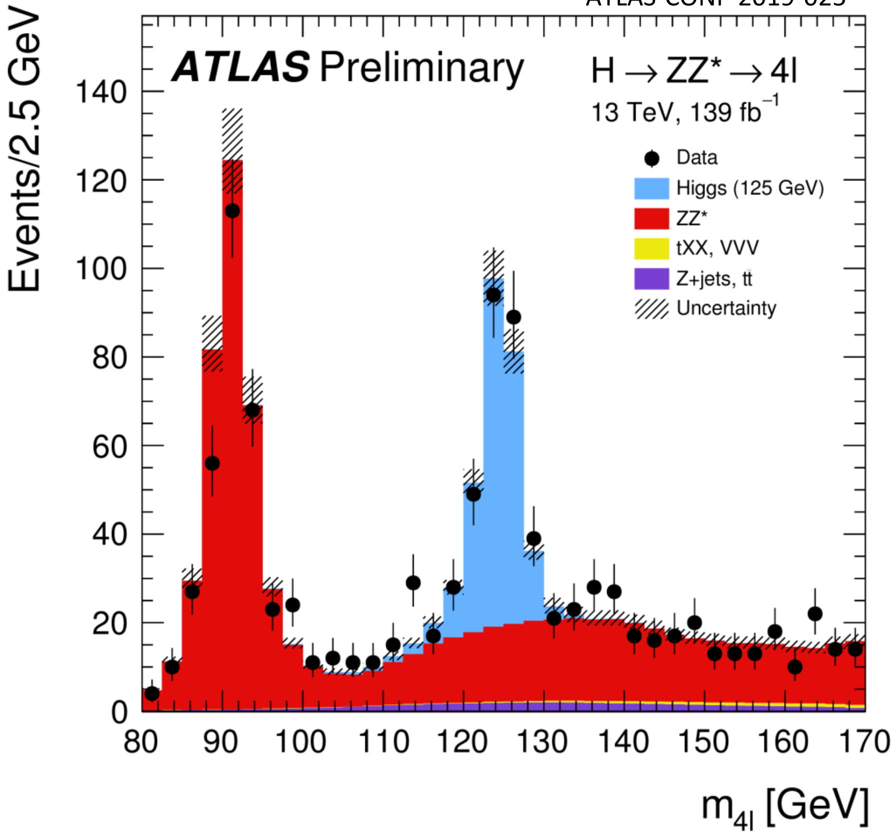

ATLAS-CONF-2019-029

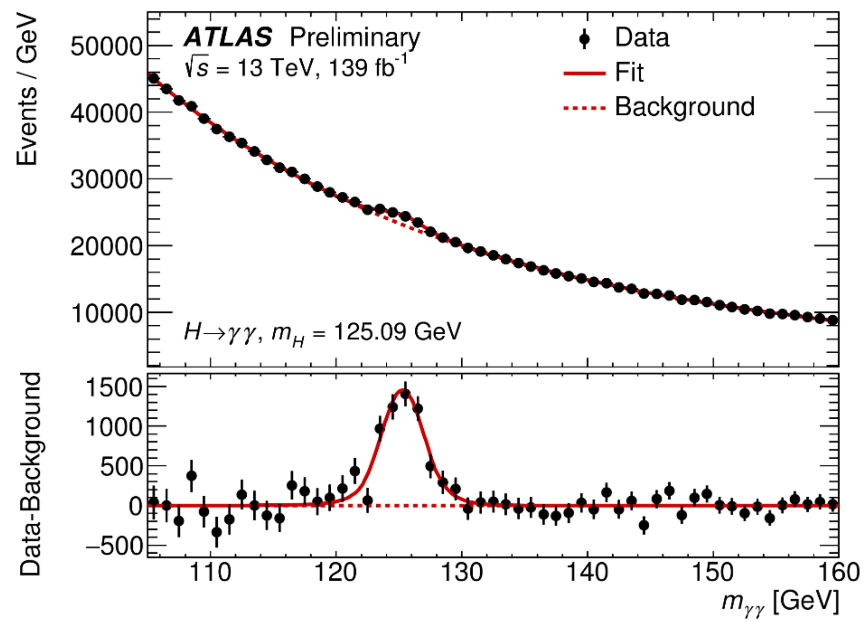

At the cost of lots of pileup

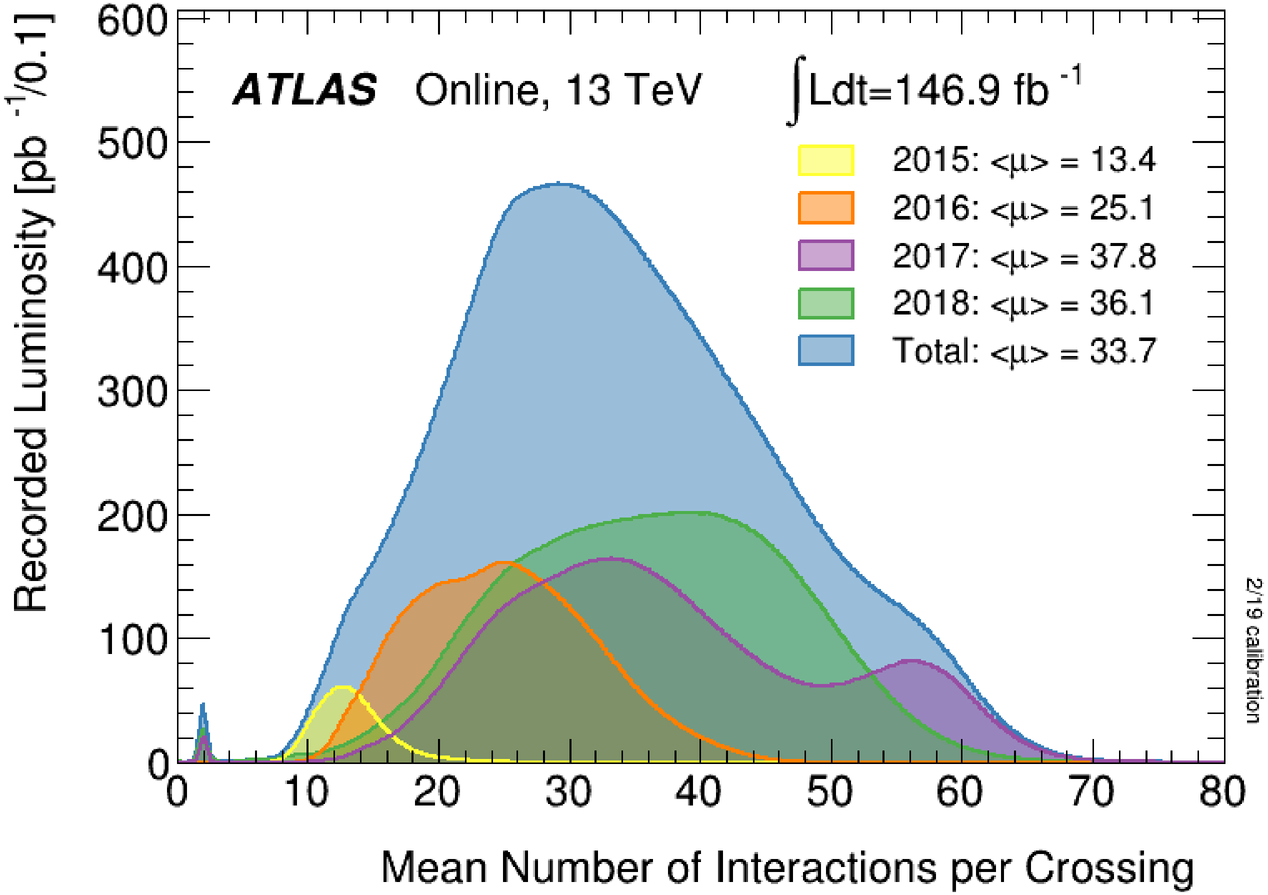

Excellent reconstruction is still possible (with innovation)

ATLAS-CONF-2018-038

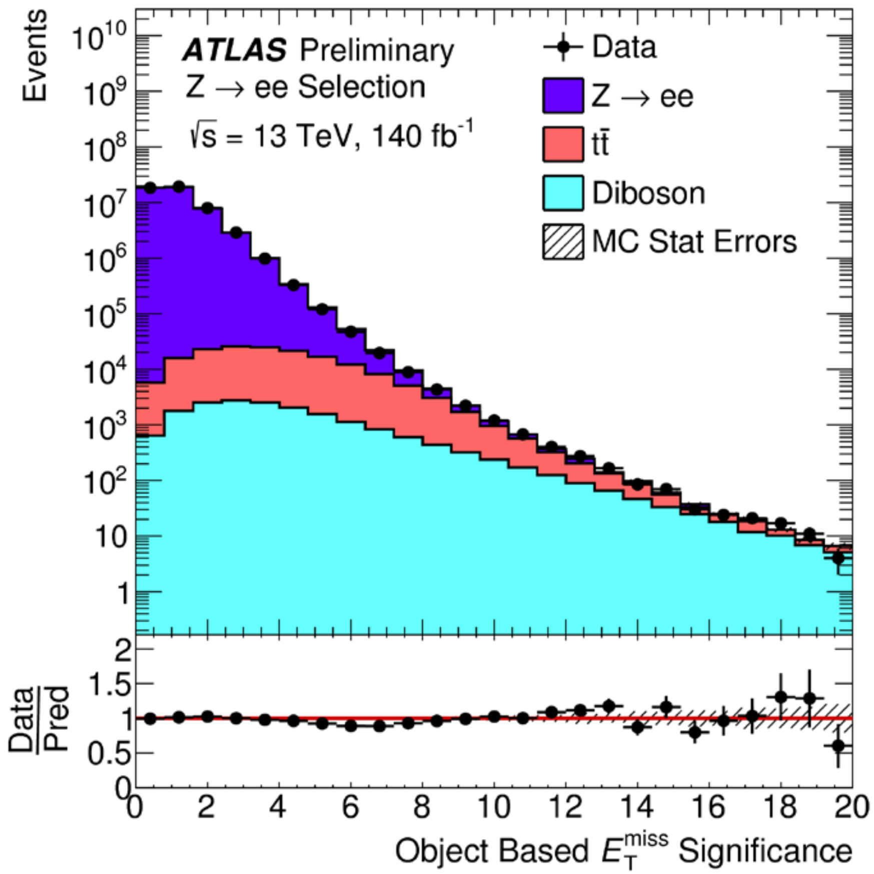

Example: **missing momentum**

- Calculate resolution for each visible object
- Find likelihood that the vector sum differs from zero

$$\mathcal{S}^2 = 2\ \ln\left(\frac{\mathcal{L}(\boldsymbol{E}_{\mathrm{T}}^{\mathrm{miss}} | \boldsymbol{E}_{\mathrm{T}}^{\mathrm{miss}})}{\mathcal{L}(\boldsymbol{E}_{\mathrm{T}}^{\mathrm{miss}} | \mathbf{0})}\right)$$

$$= (\boldsymbol{E}_{\mathrm{T}}^{\mathrm{miss}})^{\mathrm{T}} \left(\sum_i \mathbf{V}^i\right)^{-1} (\boldsymbol{E}_{\mathrm{T}}^{\mathrm{miss}})$$

$$\mathcal{L} = -\frac{1}{4} F_{\mu\nu} F^{\mu\nu} + i \bar{\Psi} \not{D} \psi + h.c. + \bar{\Psi}_i y_{ij} \psi_j \phi + h.c. + |D_\mu \phi|^2 - V(\phi)$$

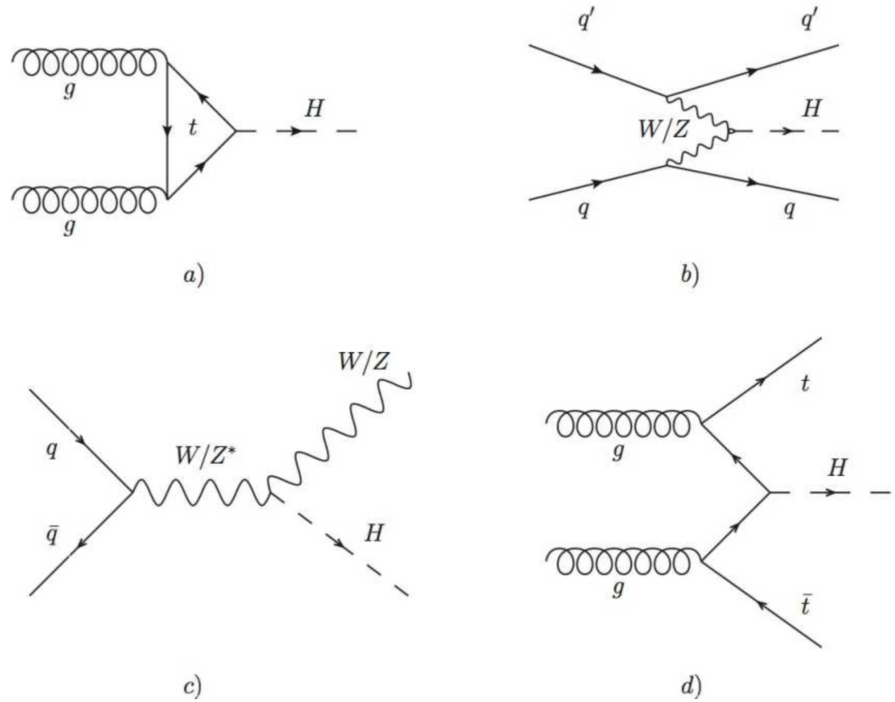

Making and breaking them

As of Scalars 2017

Production

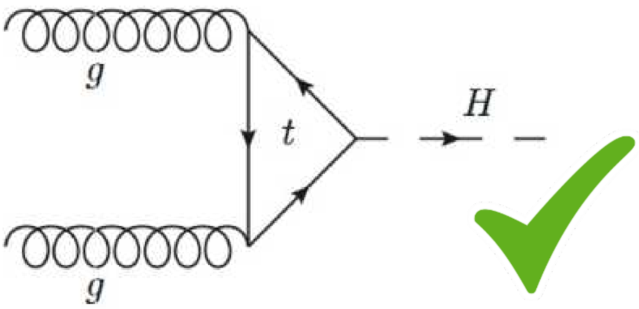

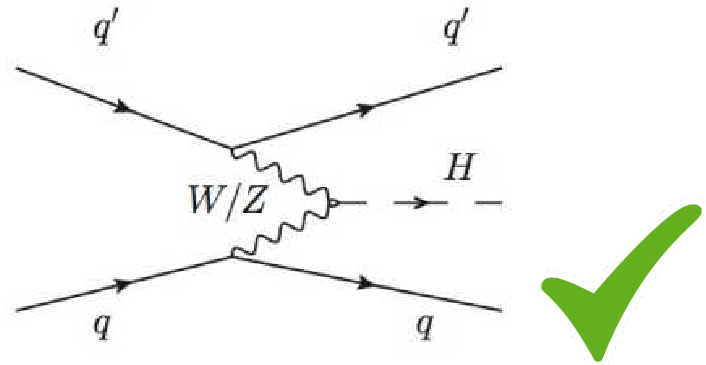

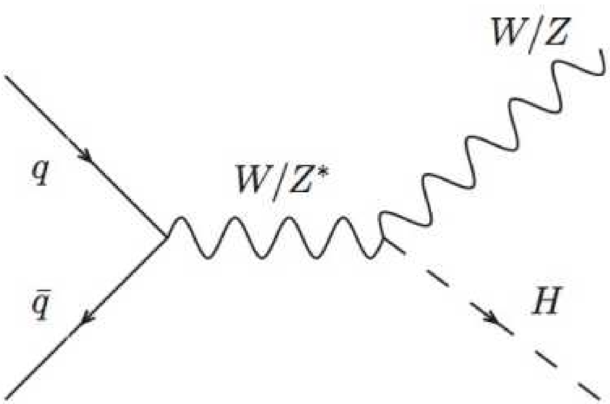

3.5σ evidence

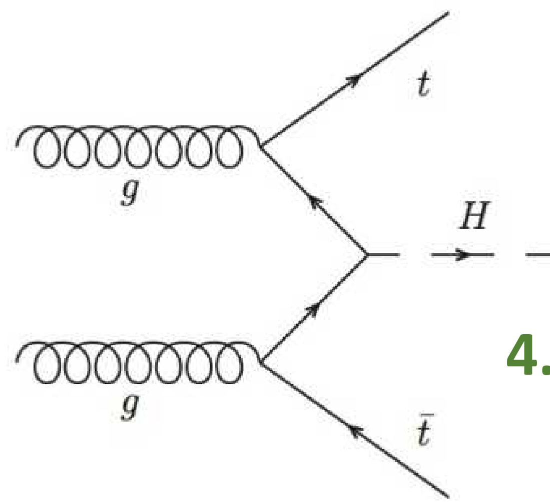

4.2σ

As of Scalars 2017

Decay

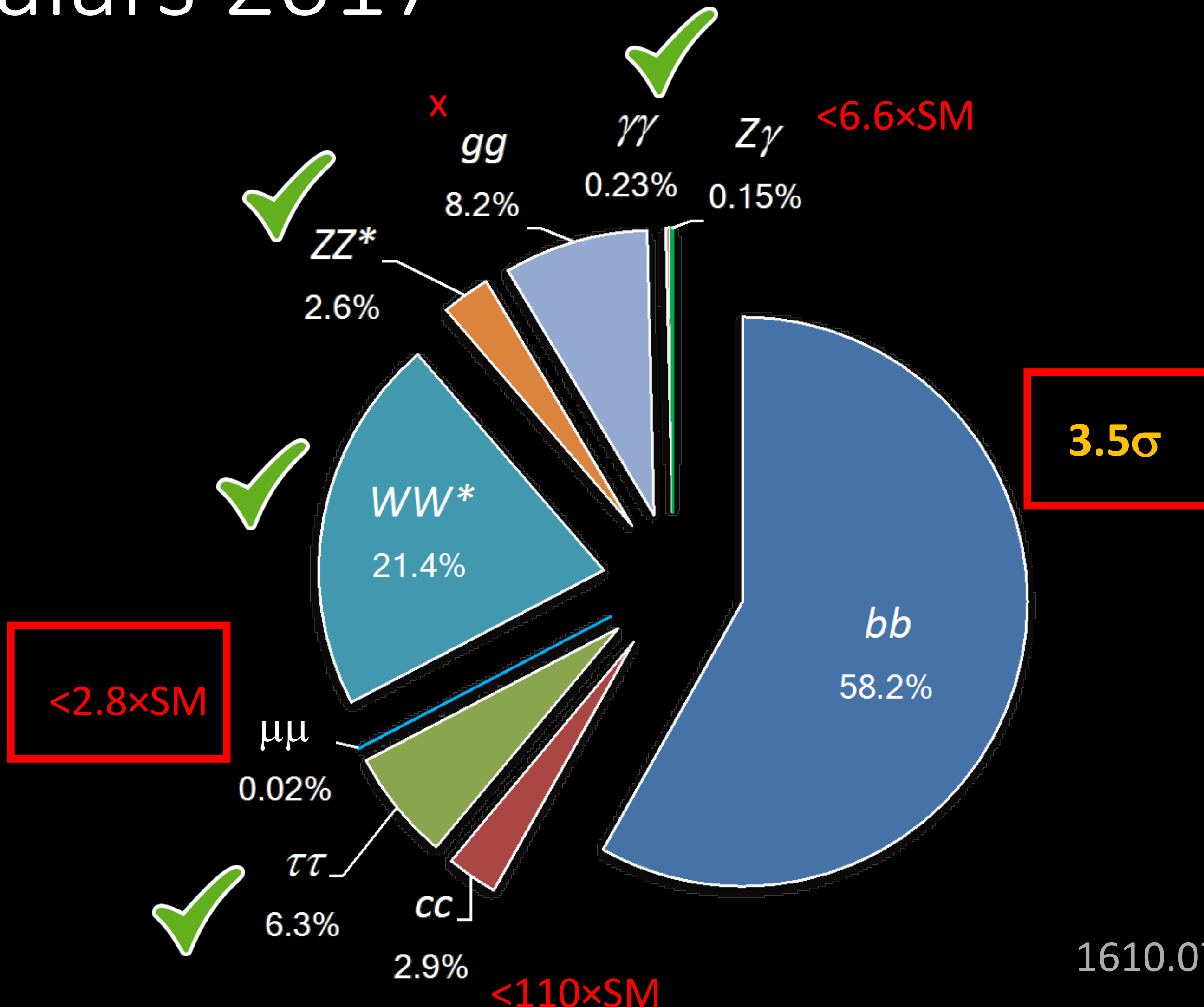

1610.07922

Towards H→ bb

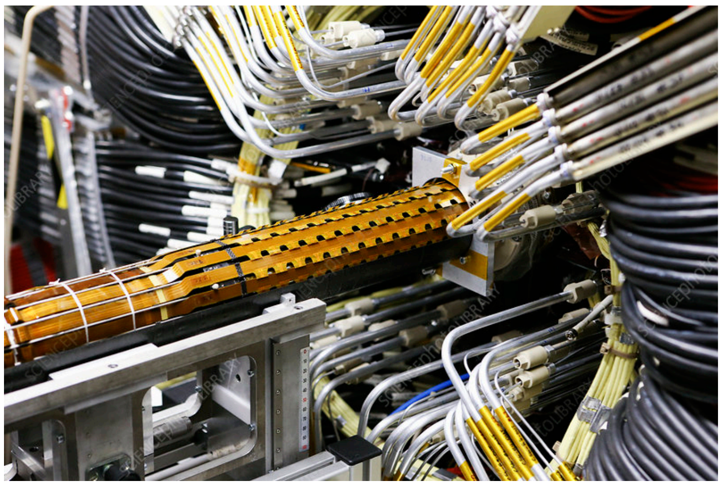

Previously:
b-layer added
before Run-2

1907.05120

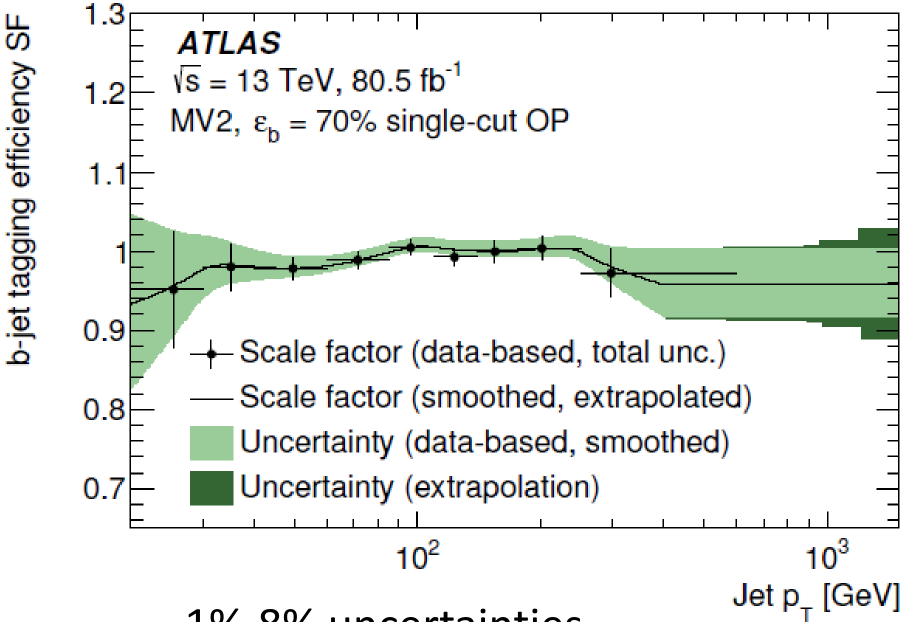

1%-8% uncertainties

b-tagging measured
using tt events

VH & H→ bb

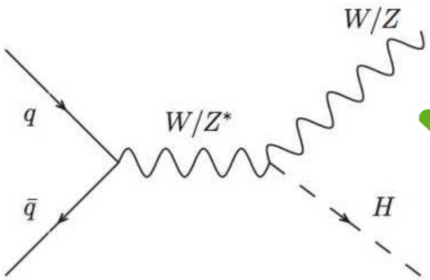

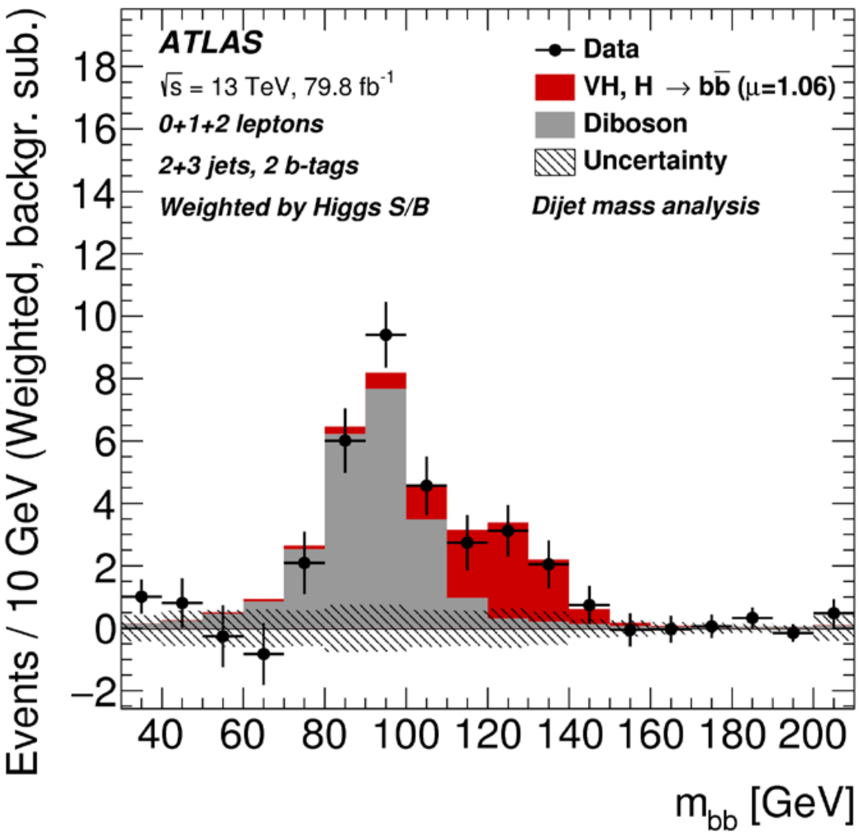

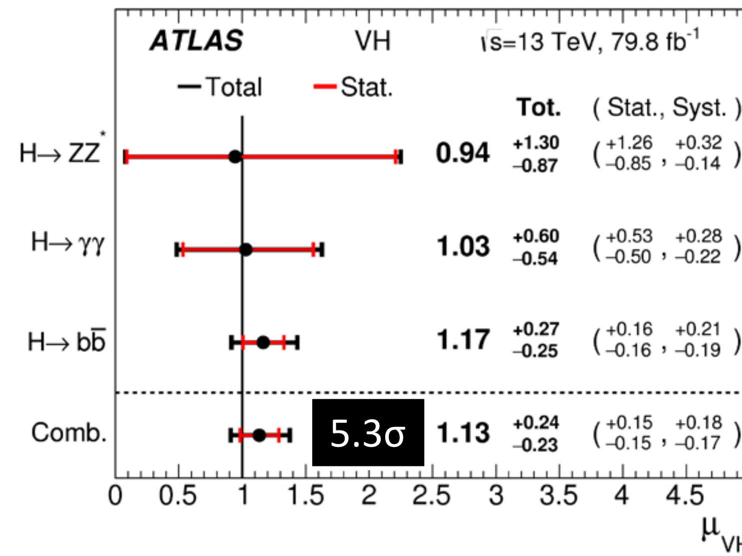

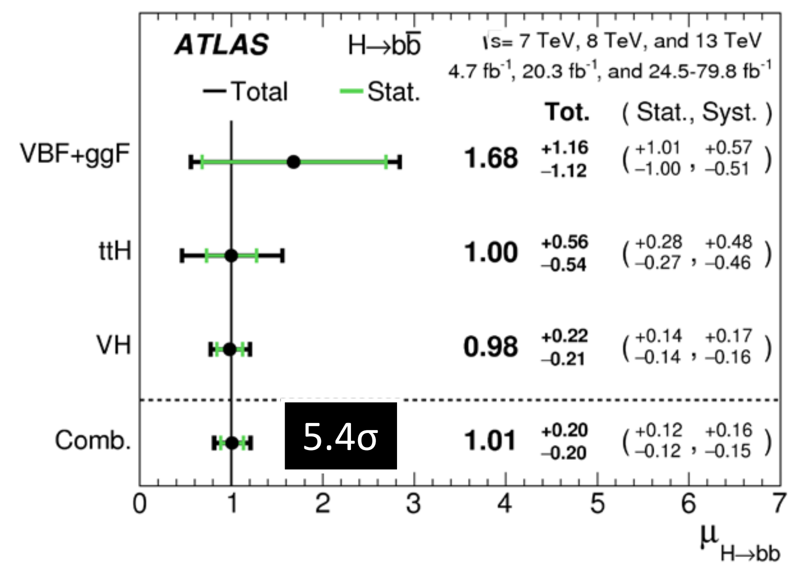

VH production and bb decay both observed

Observation of ttH production

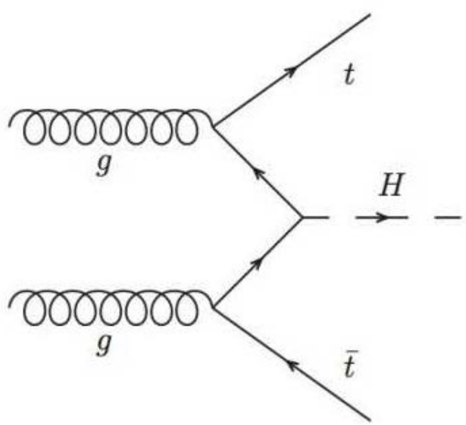

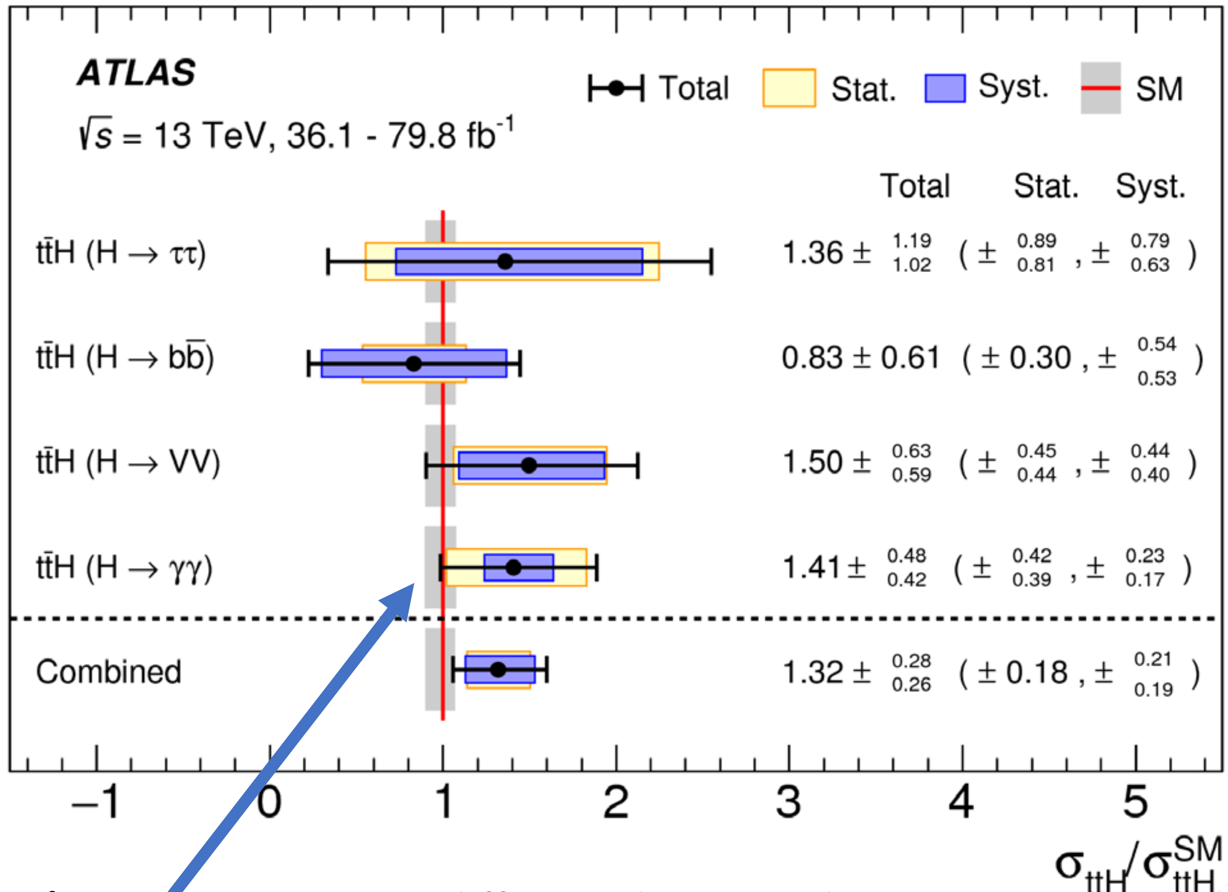

Photon identification and diphoton resolution were key

Four different decay modes contributed to ttH observation

6.3 σ observation

Observation of ttH production

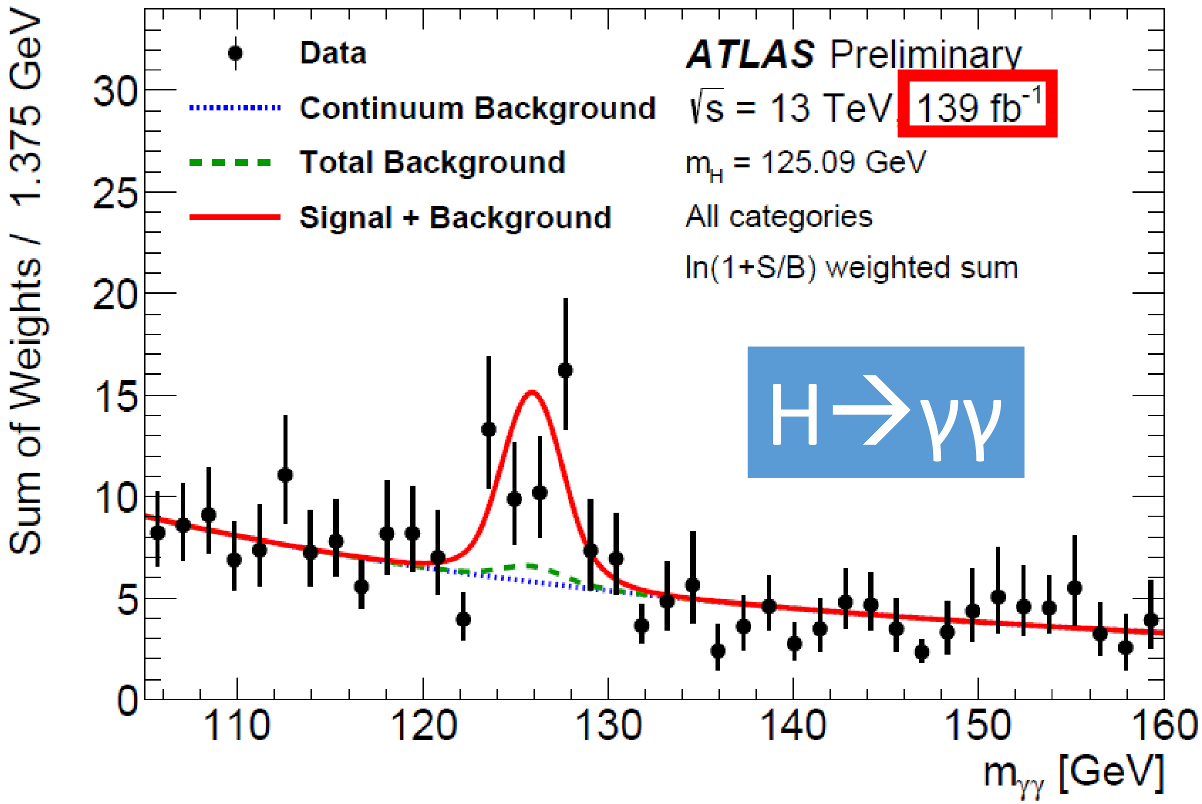

4.9σ in a single decay channel

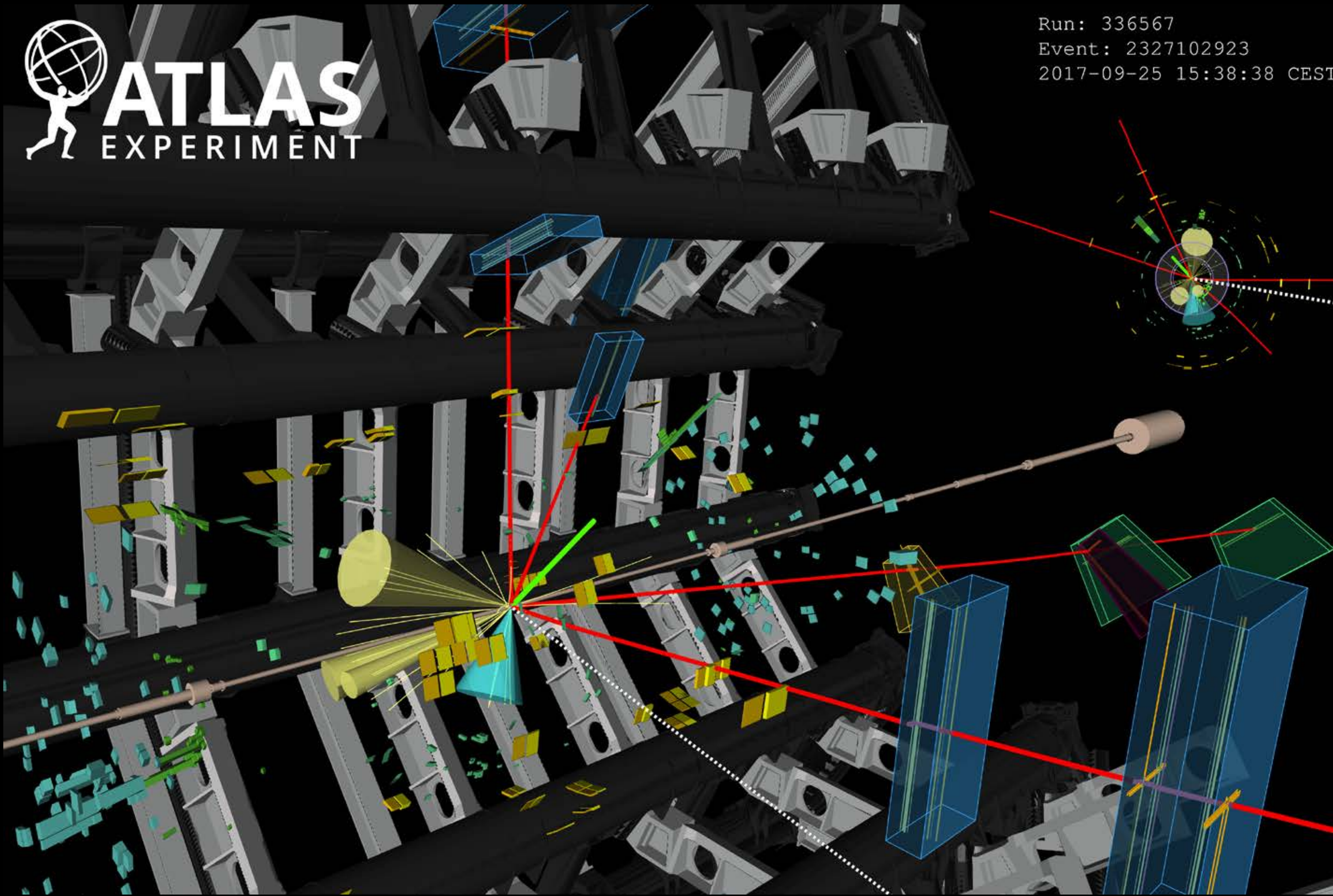

Display of a tt(→e+jets)+H(→μμμμ) candidate https://atlas.web.cern.ch/Atlas/GROUPS/PHYSICS/CombinedSummaryPlots/HIGGS/

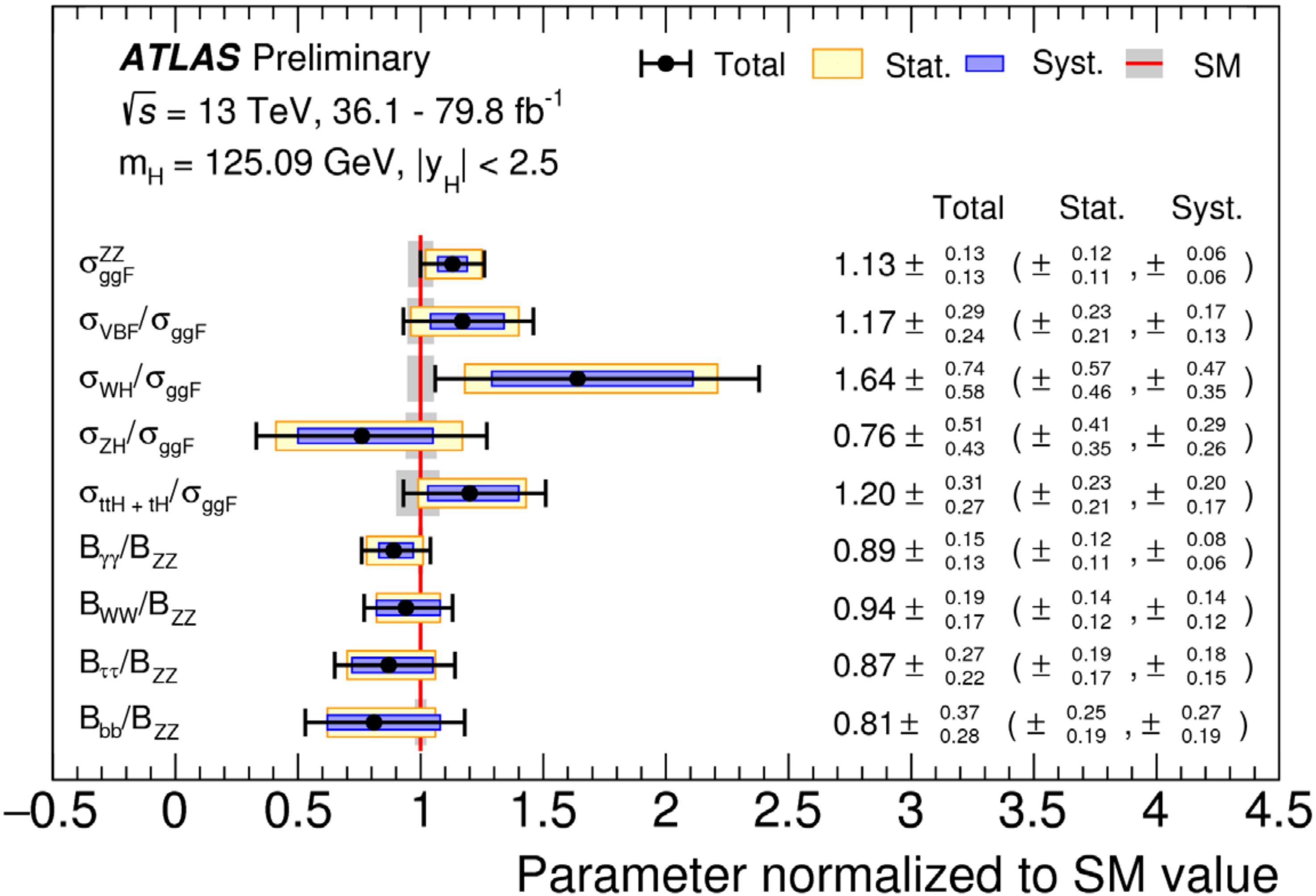

Summary of some production and decay mode measurements

Probing the small couplings

$H \to \mu\mu$

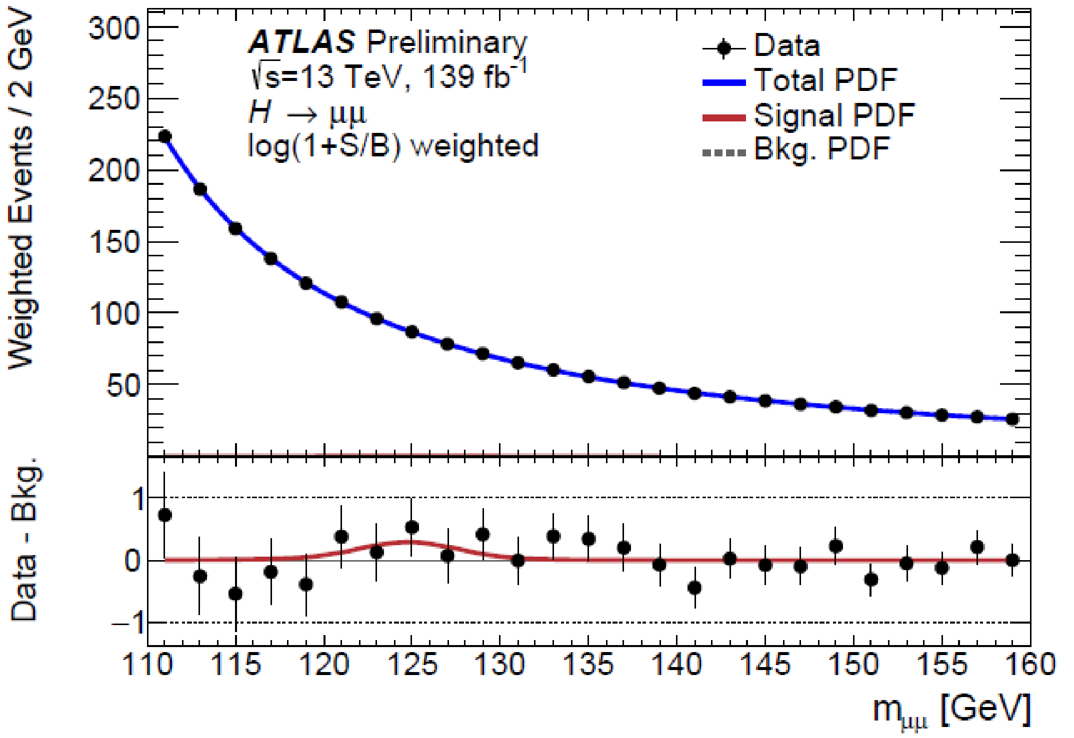

$BR_{SM} = 2.2 \times 10^{-4}$

$$\mu = 0.5 \pm 0.7$$

$$\mathrm{Br}(H \to \mu\mu) < 3.8 \cdot 10^{-4}$$

Upper limit on the signal strength: **1.7**
(expect 1.3 for the case of no signal)

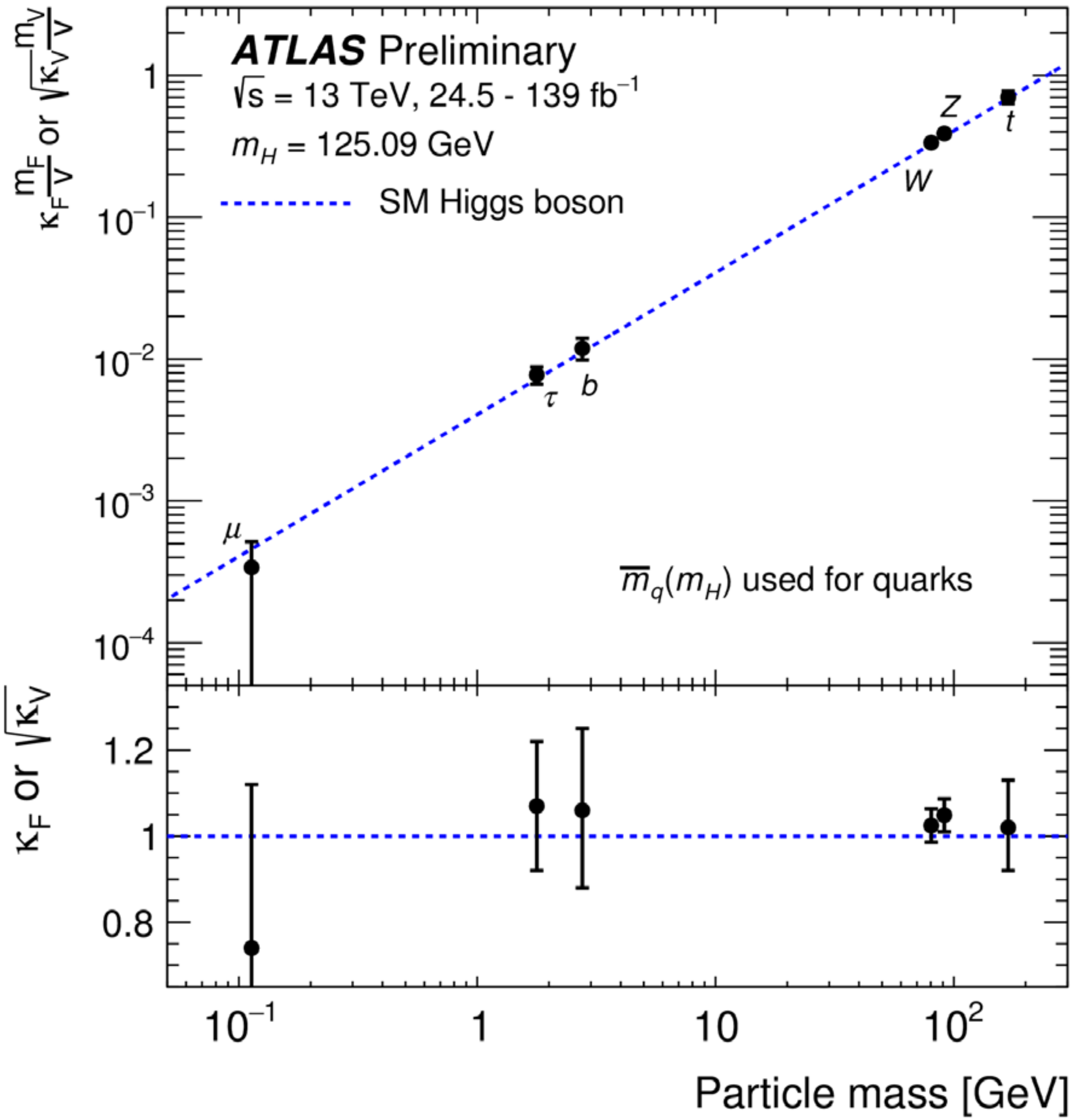
ATLAS Preliminary
√s = 13 TeV, 24.5 - 139 fb⁻¹
m_H = 125.09 GeV
SM Higgs boson
$\overline{m}_q(m_H)$ used for quarks
μ
τ
b
W
Z
t
$\kappa_F \frac{m_F}{v}$ or $\sqrt{\kappa_V}\frac{m_V}{v}$
κ_F or $\sqrt{\kappa_V}$
Particle mass [GeV]

Electron modes

$BR_{SM} \approx 5 \times 10^{-9}$

ee

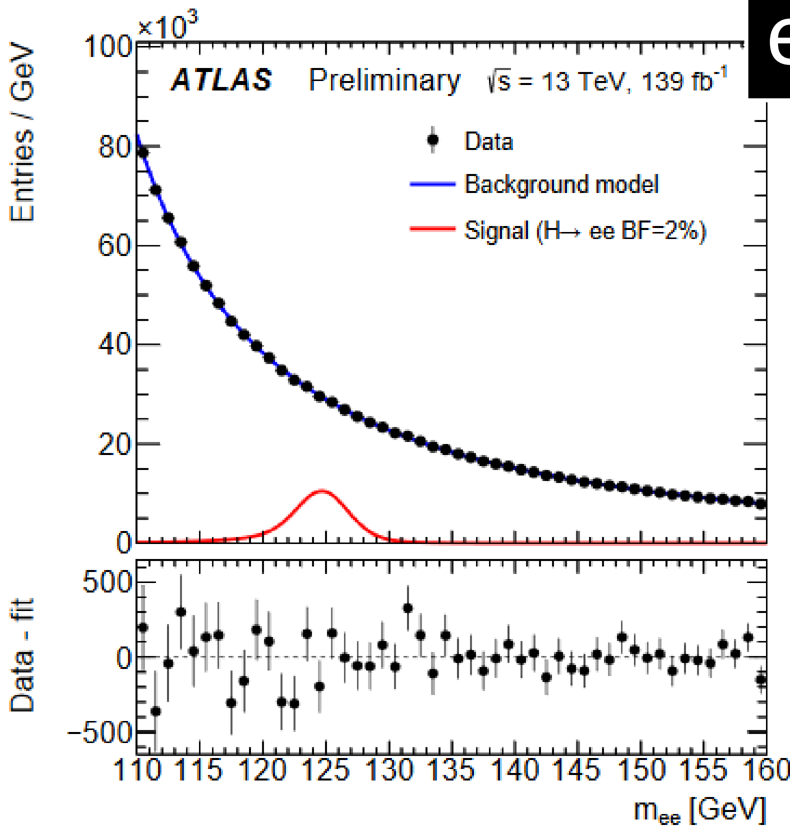

BR < 3.6×10^{-4}

$BR_{SM} \approx 0$

eμ

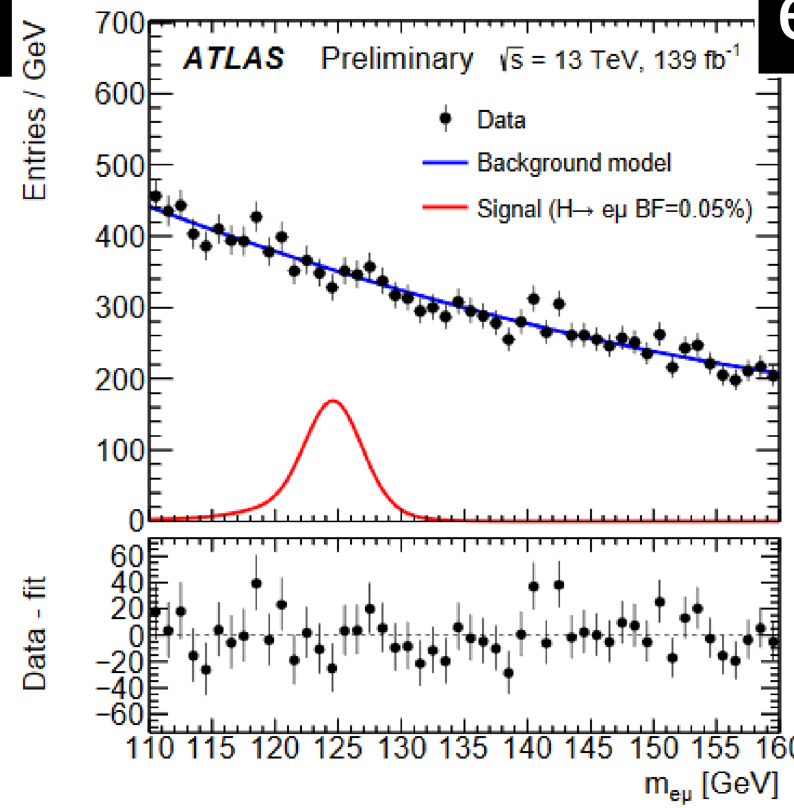

BR < 6.1×10^{-5}

More flavour-violating modes

More signal-like

eτ

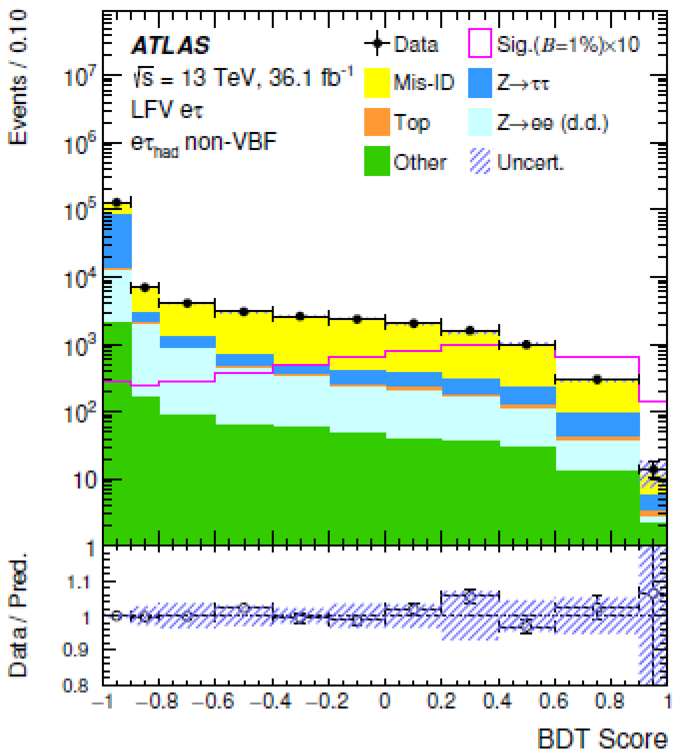

BR < 0.47%

More signal-like

μτ

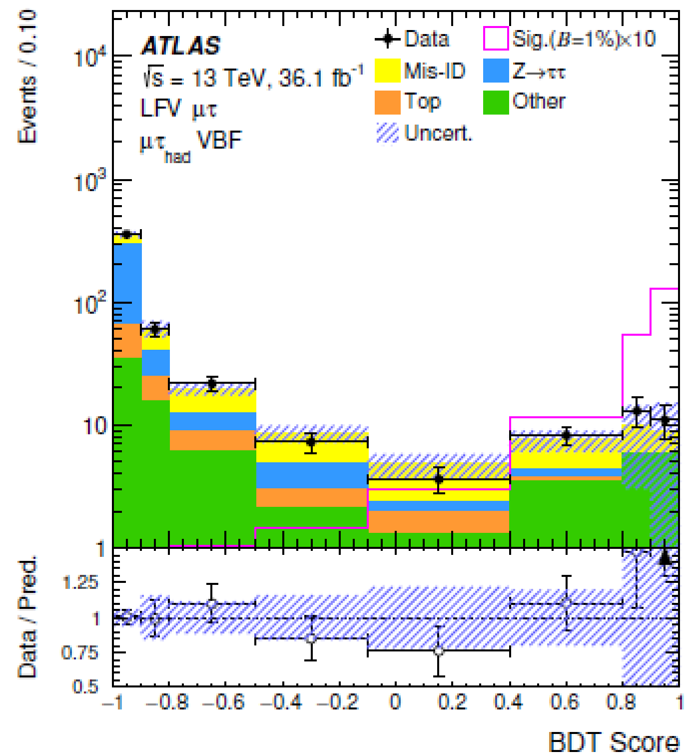

BR < 0.28%

Example signal region BDT scores

λHHH self-coupling

$$V(H^\dagger H) = \mu^2 H^\dagger H + \eta (H^\dagger H)^2$$
$$\rightarrow \frac{1}{2} m_h^2 h^2 + \sqrt{\frac{\eta}{2}} m_h h^3 + \frac{\eta}{4} h^4 \,,$$

Direct HH searches

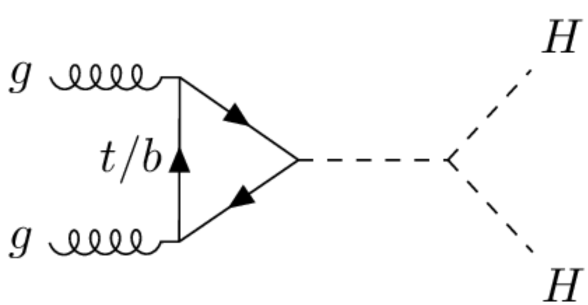

Loop effects

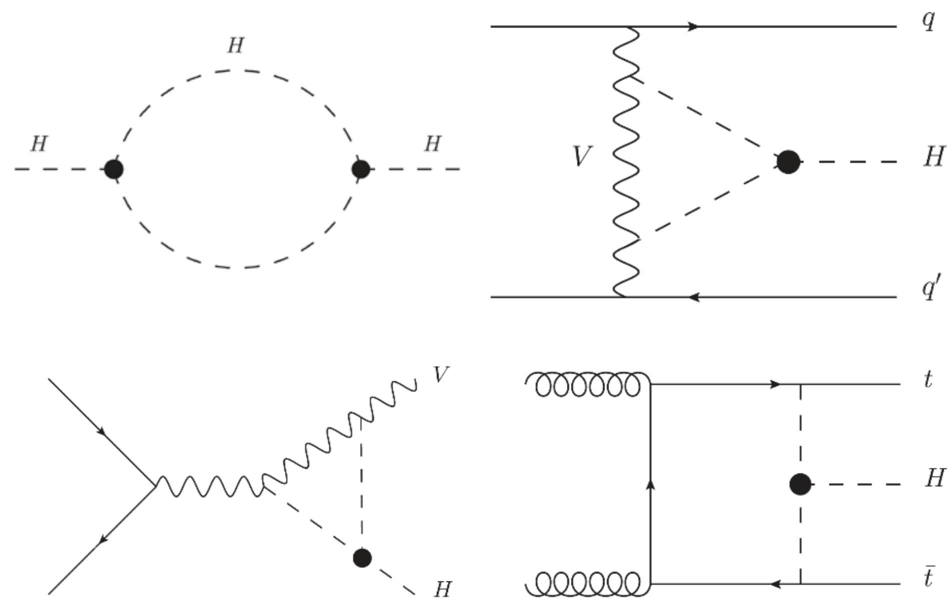

λHHH self-coupling

HH production

1906.02025

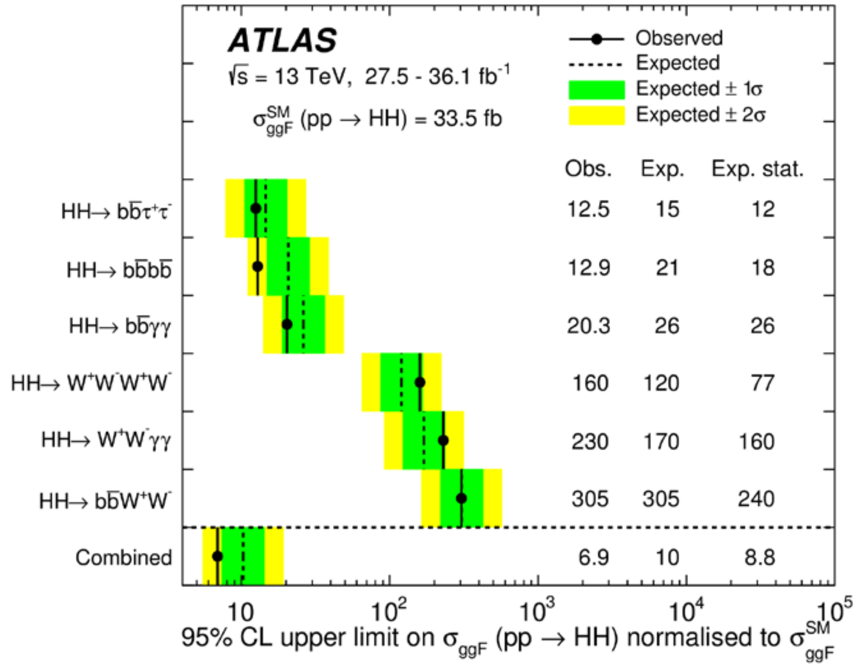

1906.02025

	Allowed κ_λ interval at 95% CL		
Final state	Obs.	Exp.	Exp. stat.
$b\bar{b}b\bar{b}$	−10.9 — 20.1	−11.6 — 18.8	−9.8 — 16.3
$b\bar{b}\tau^+\tau^-$	−7.4 — 15.7	−8.9 — 16.8	−7.8 — 15.5
$b\bar{b}\gamma\gamma$	−8.1 — 13.1	−8.1 — 13.1	−7.9 — 12.9
Combination	−5.0 — 12.0	−5.8 — 12.0	−5.3 — 11.5

Loop effects

ATL-PHYS-PUB-2019-009

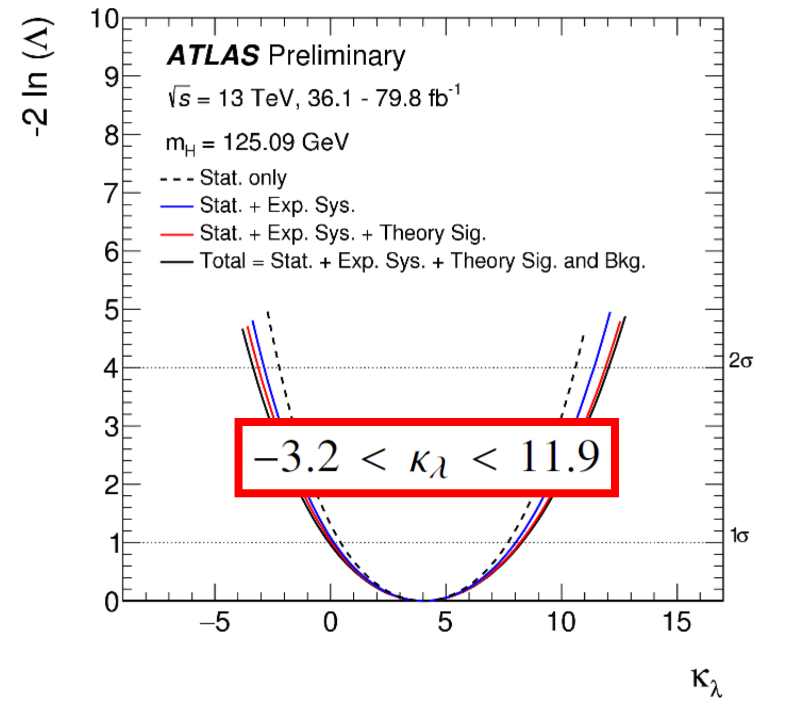

See also:

HH→bbWW (139/fb)
(1908.06765)

Φ → HH → bbbb (VBF) 126/fb
(ATLAS-CONF-2019-030)

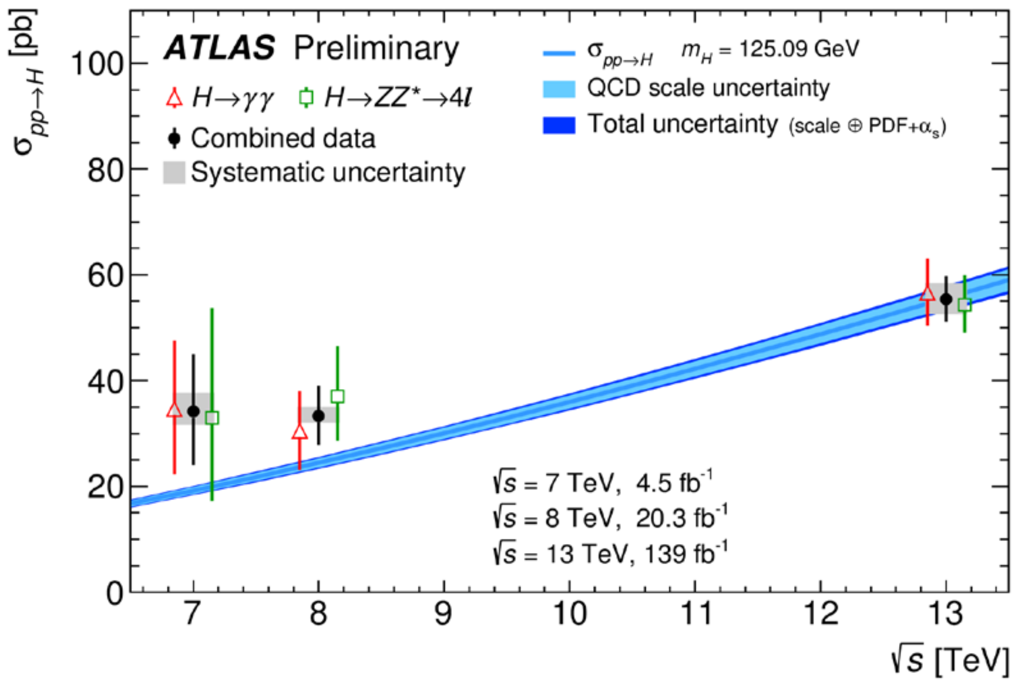

Measure measure measure

Differential distributions

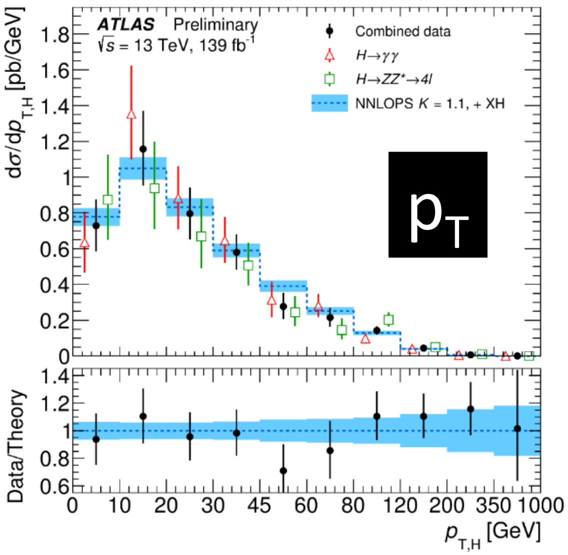

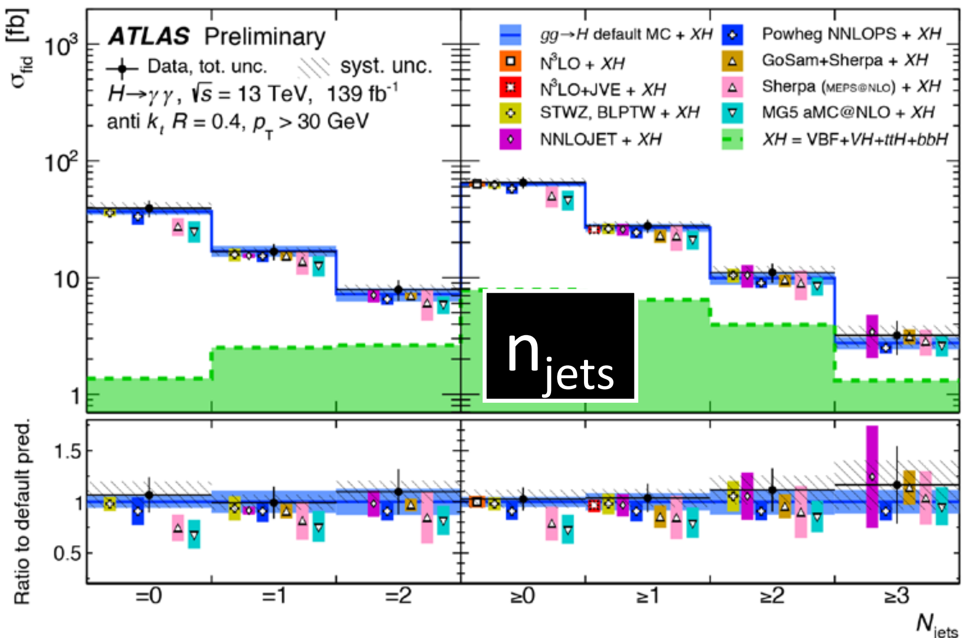

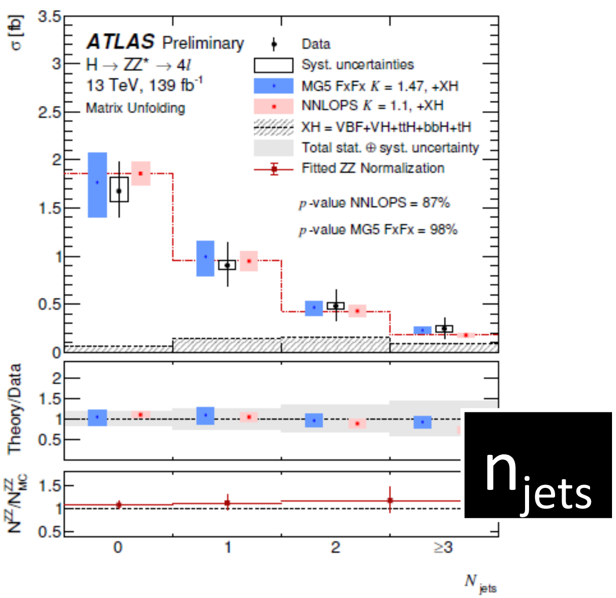

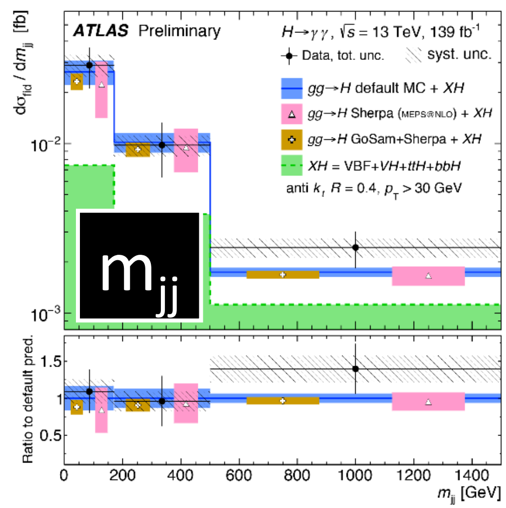

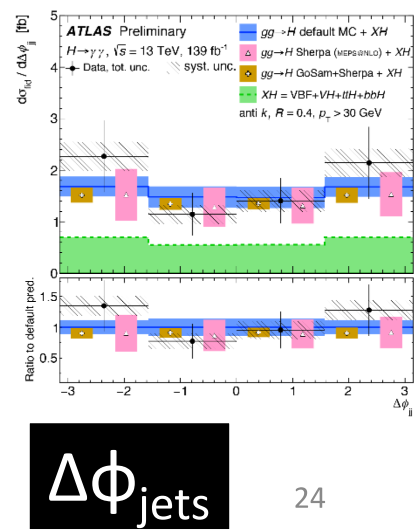

EFT constraints

1008.4884
Grzadkowski et al

X^3		φ^6 and $\varphi^4 D^2$		$\psi^2\varphi^3$	
Q_G	$f^{ABC} G_\mu^{A\nu} G_\nu^{B\rho} G_\rho^{C\mu}$	Q_φ	$(\varphi^\dagger\varphi)^3$	$Q_{e\varphi}$	$(\varphi^\dagger\varphi)(\bar l_p e_r \varphi)$
$Q_{\widetilde G}$	$f^{ABC} \widetilde G_\mu^{A\nu} G_\nu^{B\rho} G_\rho^{C\mu}$	$Q_{\varphi\Box}$	$(\varphi^\dagger\varphi)\Box(\varphi^\dagger\varphi)$	$Q_{u\varphi}$	$(\varphi^\dagger\varphi)(\bar q_p u_r \widetilde\varphi)$
Q_W	$\varepsilon^{IJK} W_\mu^{I\nu} W_\nu^{J\rho} W_\rho^{K\mu}$	$Q_{\varphi D}$	$\left(\varphi^\dagger D^\mu\varphi\right)^\star \left(\varphi^\dagger D_\mu\varphi\right)$	$Q_{d\varphi}$	$(\varphi^\dagger\varphi)(\bar q_p d_r \varphi)$
$Q_{\widetilde W}$	$\varepsilon^{IJK} \widetilde W_\mu^{I\nu} W_\nu^{J\rho} W_\rho^{K\mu}$				
$X^2\varphi^2$		$\psi^2 X\varphi$		$\psi^2\varphi^2 D$	
$Q_{\varphi G}$	$\varphi^\dagger\varphi\, G_{\mu\nu}^A G^{A\mu\nu}$	Q_{eW}	$(\bar l_p \sigma^{\mu\nu} e_r)\tau^I \varphi W_{\mu\nu}^I$	$Q_{\varphi l}^{(1)}$	$(\varphi^\dagger i\overleftrightarrow{D}_\mu \varphi)(\bar l_p \gamma^\mu l_r)$
$Q_{\varphi\widetilde G}$	$\varphi^\dagger\varphi\, \widetilde G_{\mu\nu}^A G^{A\mu\nu}$	Q_{eB}	$(\bar l_p \sigma^{\mu\nu} e_r)\varphi B_{\mu\nu}$	$Q_{\varphi l}^{(3)}$	$(\varphi^\dagger i\overleftrightarrow{D}_\mu^I \varphi)(\bar l_p \tau^I \gamma^\mu l_r)$
$Q_{\varphi W}$	$\varphi^\dagger\varphi\, W_{\mu\nu}^I W^{I\mu\nu}$	Q_{uG}	$(\bar q_p \sigma^{\mu\nu} T^A u_r)\widetilde\varphi\, G_{\mu\nu}^A$	$Q_{\varphi e}$	$(\varphi^\dagger i\overleftrightarrow{D}_\mu \varphi)(\bar e_p \gamma^\mu e_r)$
$Q_{\varphi\widetilde W}$	$\varphi^\dagger\varphi\, \widetilde W_{\mu\nu}^I W^{I\mu\nu}$	Q_{uW}	$(\bar q_p \sigma^{\mu\nu} u_r)\tau^I \widetilde\varphi\, W_{\mu\nu}^I$	$Q_{\varphi q}^{(1)}$	$(\varphi^\dagger i\overleftrightarrow{D}_\mu \varphi)(\bar q_p \gamma^\mu q_r)$
$Q_{\varphi B}$	$\varphi^\dagger\varphi\, B_{\mu\nu} B^{\mu\nu}$	Q_{uB}	$(\bar q_p \sigma^{\mu\nu} u_r)\widetilde\varphi\, B_{\mu\nu}$	$Q_{\varphi q}^{(3)}$	$(\varphi^\dagger i\overleftrightarrow{D}_\mu^I \varphi)(\bar q_p \tau^I \gamma^\mu q_r)$
$Q_{\varphi\widetilde B}$	$\varphi^\dagger\varphi\, \widetilde B_{\mu\nu} B^{\mu\nu}$	Q_{dG}	$(\bar q_p \sigma^{\mu\nu} T^A d_r)\varphi\, G_{\mu\nu}^A$	$Q_{\varphi u}$	$(\varphi^\dagger i\overleftrightarrow{D}_\mu \varphi)(\bar u_p \gamma^\mu u_r)$
$Q_{\varphi WB}$	$\varphi^\dagger\tau^I\varphi\, W_{\mu\nu}^I B^{\mu\nu}$	Q_{dW}	$(\bar q_p \sigma^{\mu\nu} d_r)\tau^I \varphi\, W_{\mu\nu}^I$	$Q_{\varphi d}$	$(\varphi^\dagger i\overleftrightarrow{D}_\mu \varphi)(\bar d_p \gamma^\mu d_r)$
$Q_{\varphi\widetilde WB}$	$\varphi^\dagger\tau^I\varphi\, \widetilde W_{\mu\nu}^I B^{\mu\nu}$	Q_{dB}	$(\bar q_p \sigma^{\mu\nu} d_r)\varphi\, B_{\mu\nu}$	$Q_{\varphi ud}$	$i(\widetilde\varphi^\dagger D_\mu\varphi)(\bar u_p \gamma^\mu d_r)$

Table 2: Dimension-six operators other than the four-fermion ones.

"Warsaw basis"

$$\mathcal{L}_{\rm eff}^{\rm SMEFT} \supset \overline{C}_{HG} O'_g + \overline{C}_{HW} O'_{HW} + \overline{C}_{HB} O'_{HB} + \overline{C}_{HWB} O'_{HWB} + \widetilde{C}_{HG} \widetilde{O}'_g + \widetilde{C}_{HW} \widetilde{O}'_{HW} + \widetilde{C}_{HB} \widetilde{O}'_{HB} + \widetilde{C}_{HWB} \widetilde{O}'_{HWB},$$

$$\overline{C}_i \equiv C_i v^2/\Lambda^2$$

EFT constraints

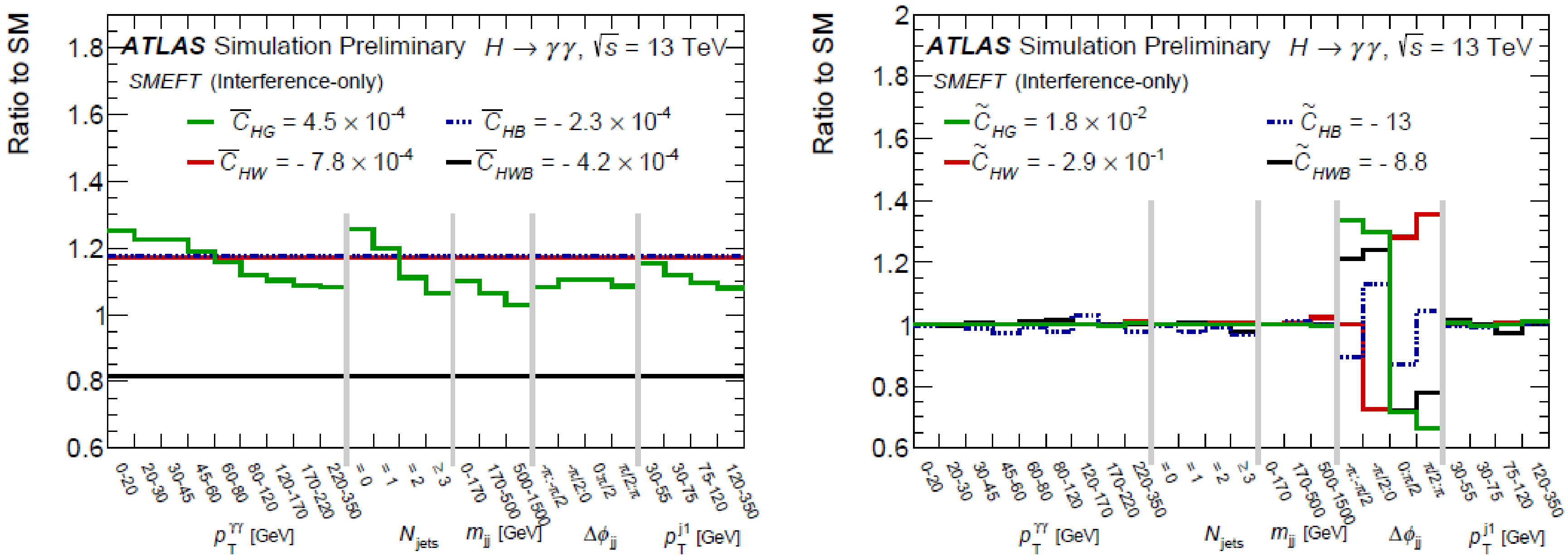

(a) (b)

Figure 10: The effect on the five differential distributions used in the analysis of (a) the CP-even coefficients $\overline{C}_{HG}$, $\overline{C}_{HB}$, $\overline{C}_{HW}$, $\overline{C}_{HWB}$ and (b) the CP-odd coefficients $\widetilde{C}_{HG}$, $\widetilde{C}_{HB}$, $\widetilde{C}_{HW}$, $\widetilde{C}_{HWB}$ of the SMEFT effective Lagrangian for values of the coefficients close to the observed limits.

EFT constraints

Table 6: The 95% CL observed limits on the $\overline{C}_{HG}$, $\overline{C}_{HW}$, $\overline{C}_{HB}$, $\overline{C}_{HWB}$ Wilson coefficients of the SMEFT basis and their CP-odd counterparts using interference-only terms and using both interference and quadratic terms. Limits are derived fitting one Wilson coefficient at a time while setting the other coefficients to zero.

Coefficient	95% CL, interference-only terms	95% CL, interference and quadratic terms
$\overline{C}_{HG}$	$[-4.2, 4.8] \times 10^{-4}$	$[-6.1, 4.7] \times 10^{-4}$
$\widetilde{C}_{HG}$	$[-2.1, 1.6] \times 10^{-2}$	$[-1.5, 1.4] \times 10^{-3}$
$\overline{C}_{HW}$	$[-8, 2, 7.4] \times 10^{-4}$	$[-8.3, 8.3] \times 10^{-4}$
$\widetilde{C}_{HW}$	$[-0.26, 0.33]$	$[-3.7, 3.7] \times 10^{-3}$
$\overline{C}_{HB}$	$[-2.4, 2.3] \times 10^{-4}$	$[-2.4, 2.4] \times 10^{-4}$
$\widetilde{C}_{HB}$	$[-13.0, 14.0]$	$[-1.2, 1.1] \times 10^{-3}$
$\overline{C}_{HWB}$	$[-4.0, 4.4] \times 10^{-4}$	$[-4.2, 4.2] \times 10^{-4}$
$\widetilde{C}_{HWB}$	$[-11.1, 6.5]$	$[-2.0, 2.0] \times 10^{-3}$

The other scalars?

Extended Higgs sector?

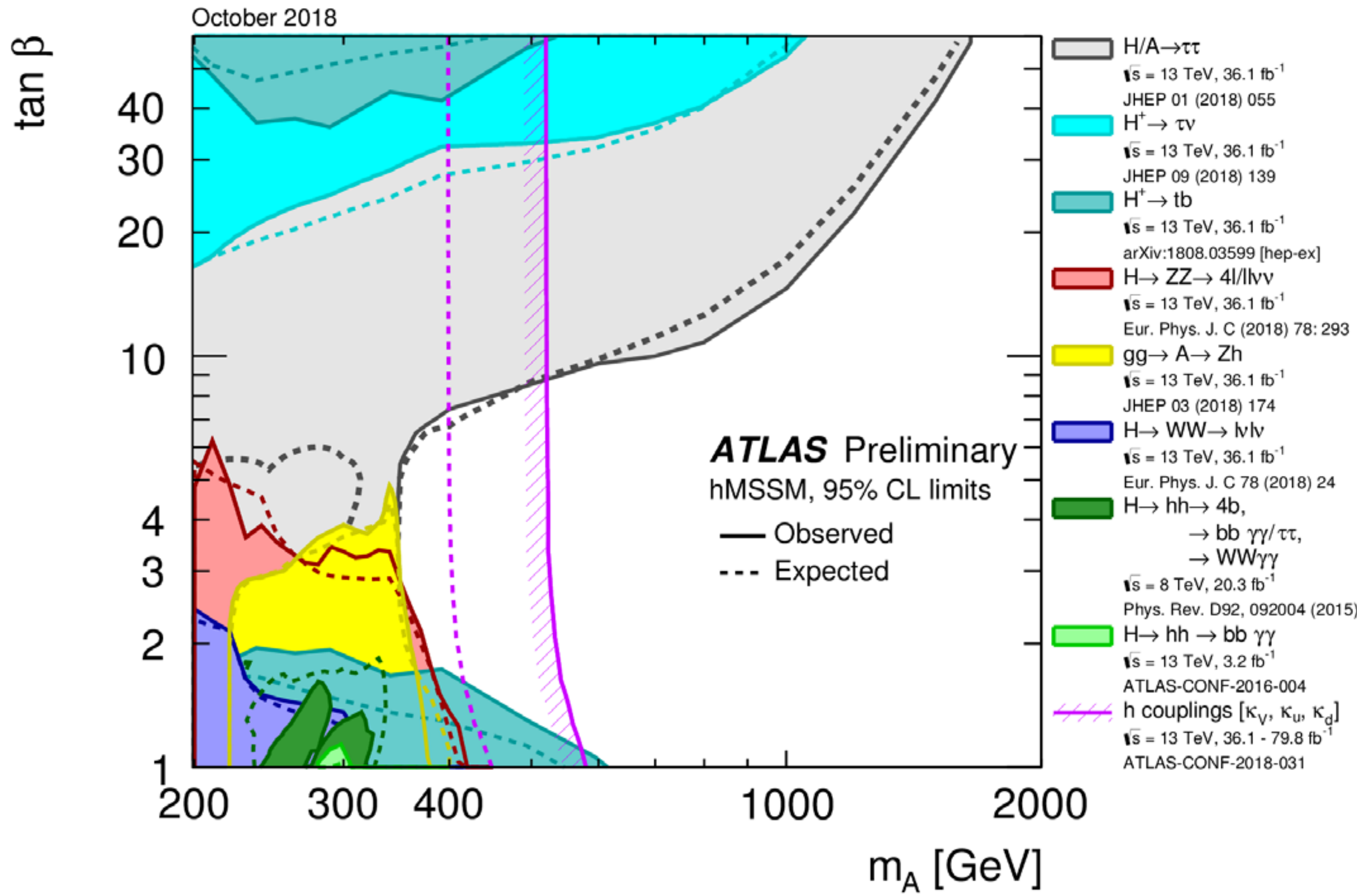

Other BSM Higgs searches (flipped 2HDM, scalar resonances, …) at:
https://twiki.cern.ch/twiki/bin/view/AtlasPublic/HDBSPublicResults

Scalar leptons?

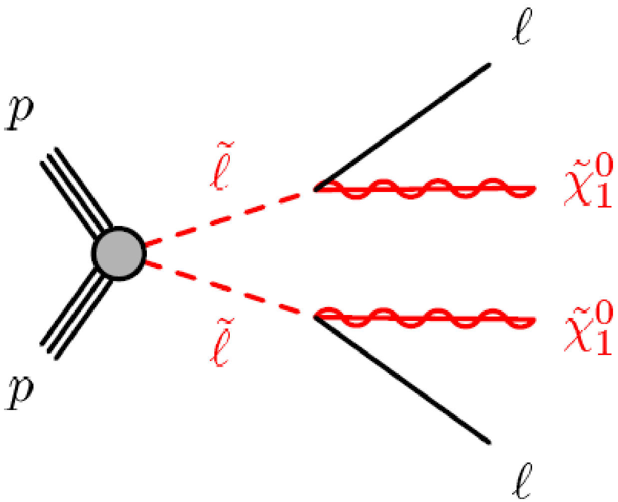

Difficult due to leptonic WW background, small cross section and low p_T leptons

This region particularly interesting for

- DM relic density
- g_μ-2

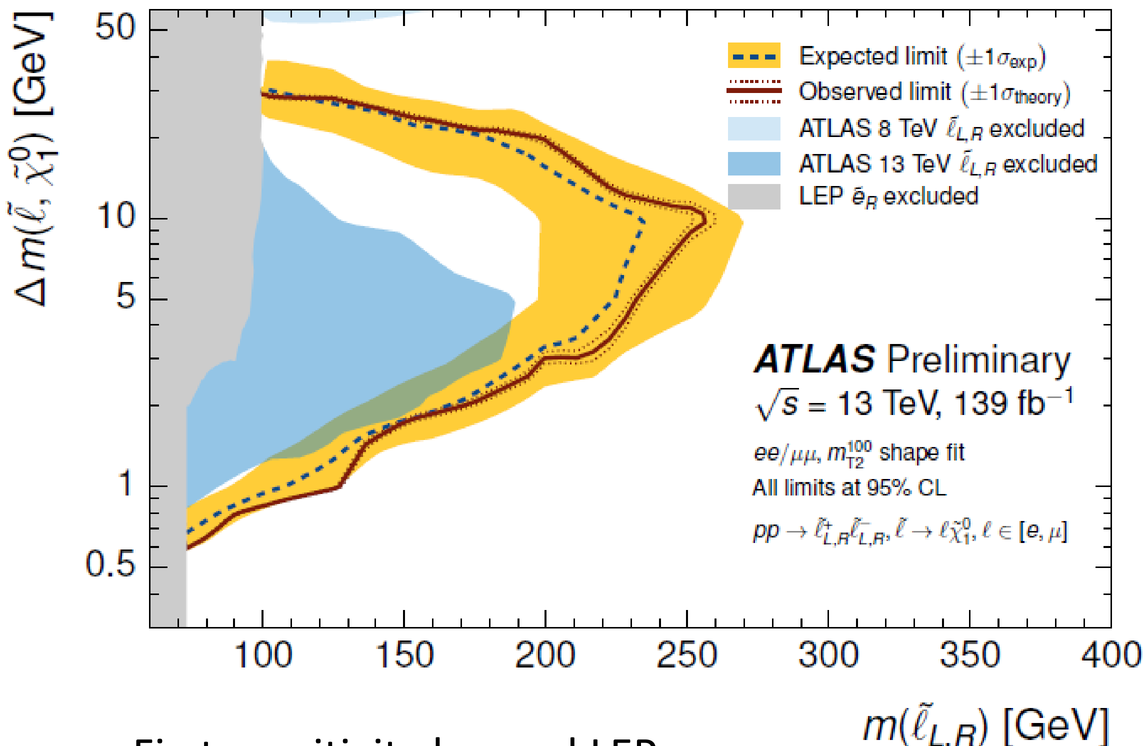

First sensitivity beyond LEP

First sensitivity to staus

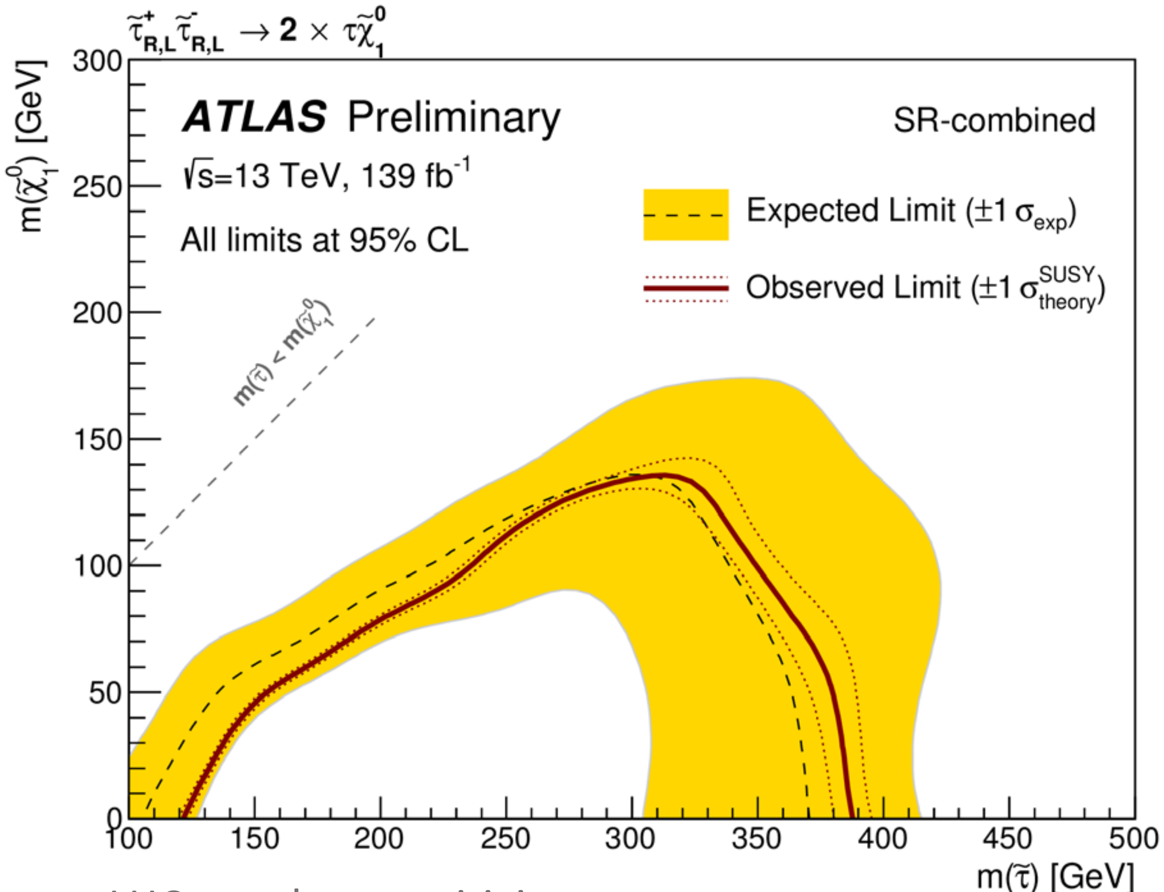

LHC now has sensitivity

Many more SUSY searches (stops, sbottoms, …) at
https://twiki.cern.ch/twiki/bin/view/AtlasPublic/SupersymmetryPublicResults

Long lived scalars

Trigger on narrow jets in HCAL (little ECAL & no tracks)

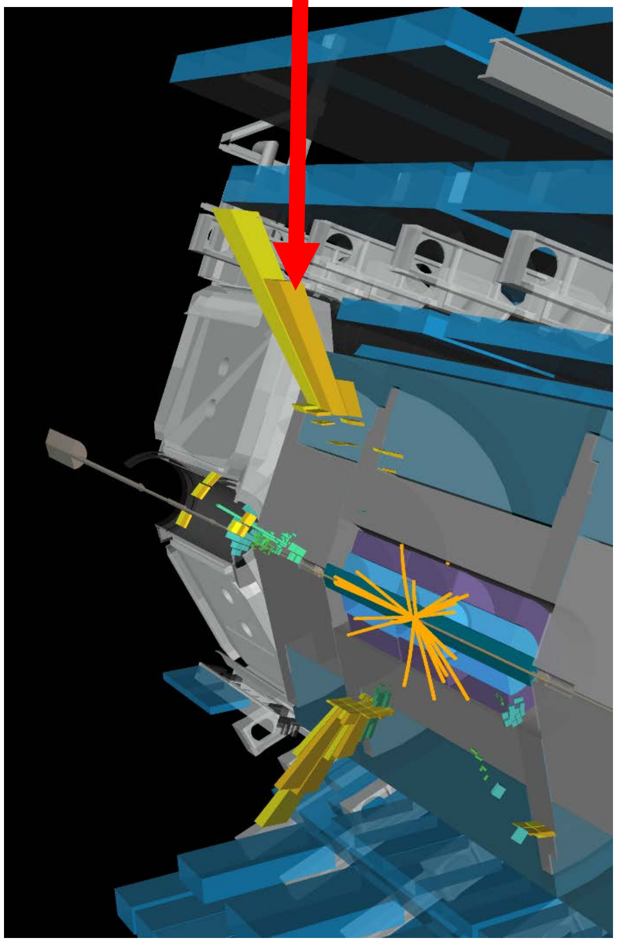

$$\Phi \to ss \to f\bar{f}f'\bar{f}'$$

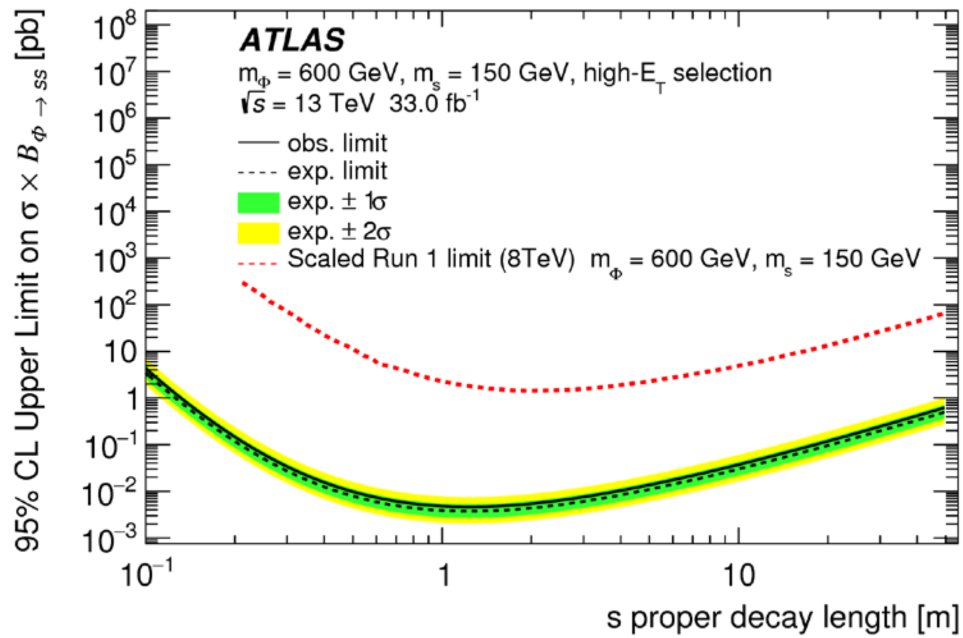

Many more exotic scalar searches (leptoquarks, dark scalars, …) can be found at: https://twiki.cern.ch/twiki/bin/view/AtlasPublic/ExoticsPublicResults

Light-by-light scattering

1904.03536

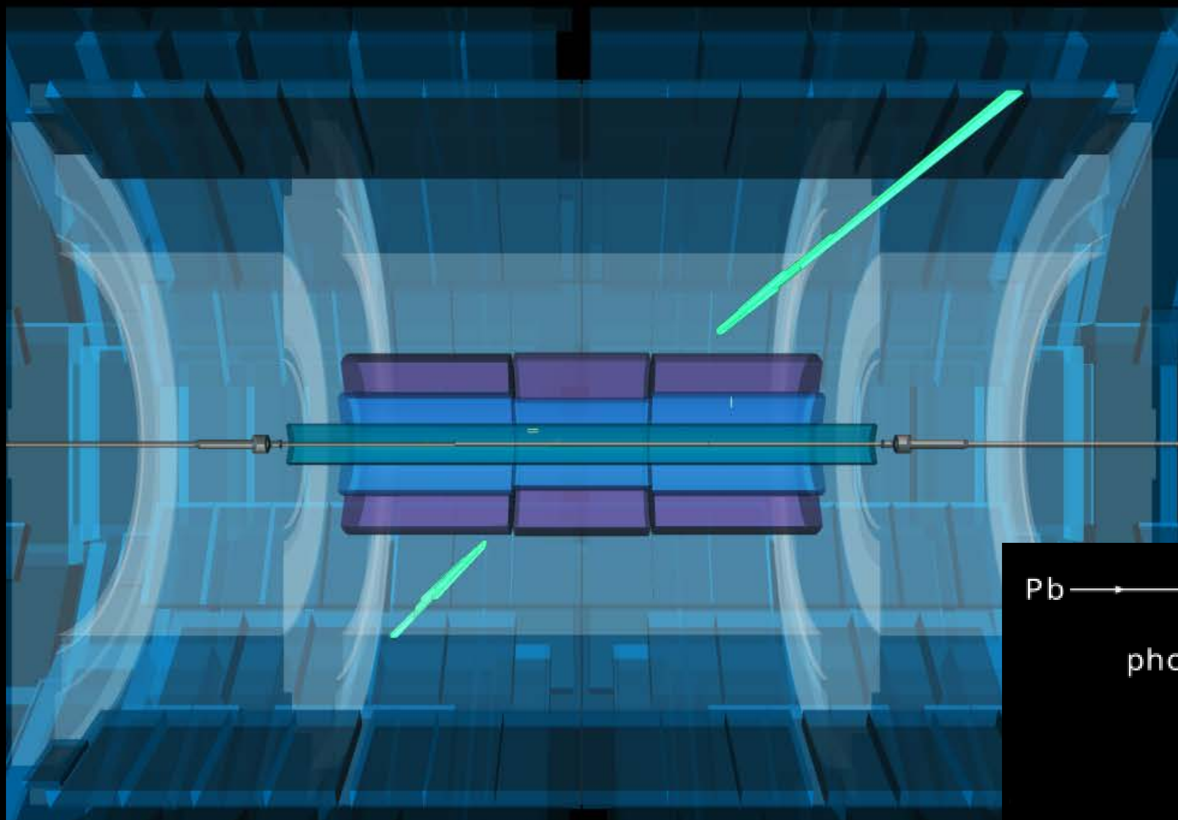

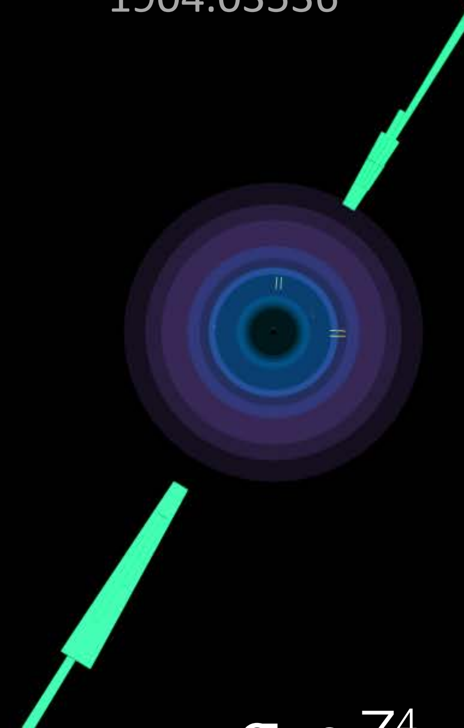

$\sigma \propto Z^4$

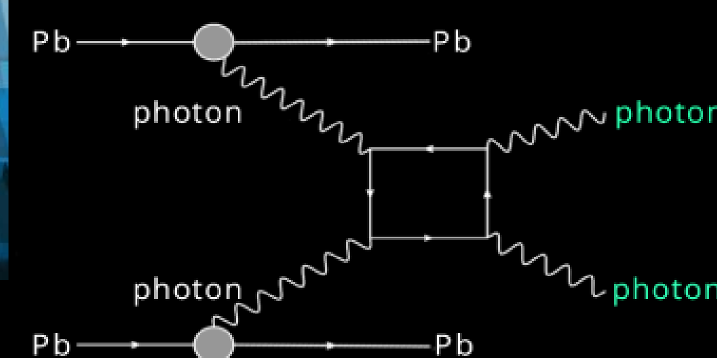

59 $\gamma\gamma \to \gamma\gamma$ events observed for
12 ± 3 expected background (8.2σ)

Conclusion

- Run-2 data-taking was a great success
- **VH** and **ttH** production are now observed
- **H→bb** decay is now observed
- **Second** generation couplings getting closer
- Rare and flavour-violating decays being tested
- Differential distributions used to test **EFT**s
- **Searches** continue on a broad front

Lots more results at:
https://twiki.cern.ch/twiki/bin/view/AtlasPublic/

MERTON COLLEGE
OXFORD

Science & Technology
Facilities Council

UNIVERSITY OF
OXFORD

ATLAS
EXPERIMENT

Mass

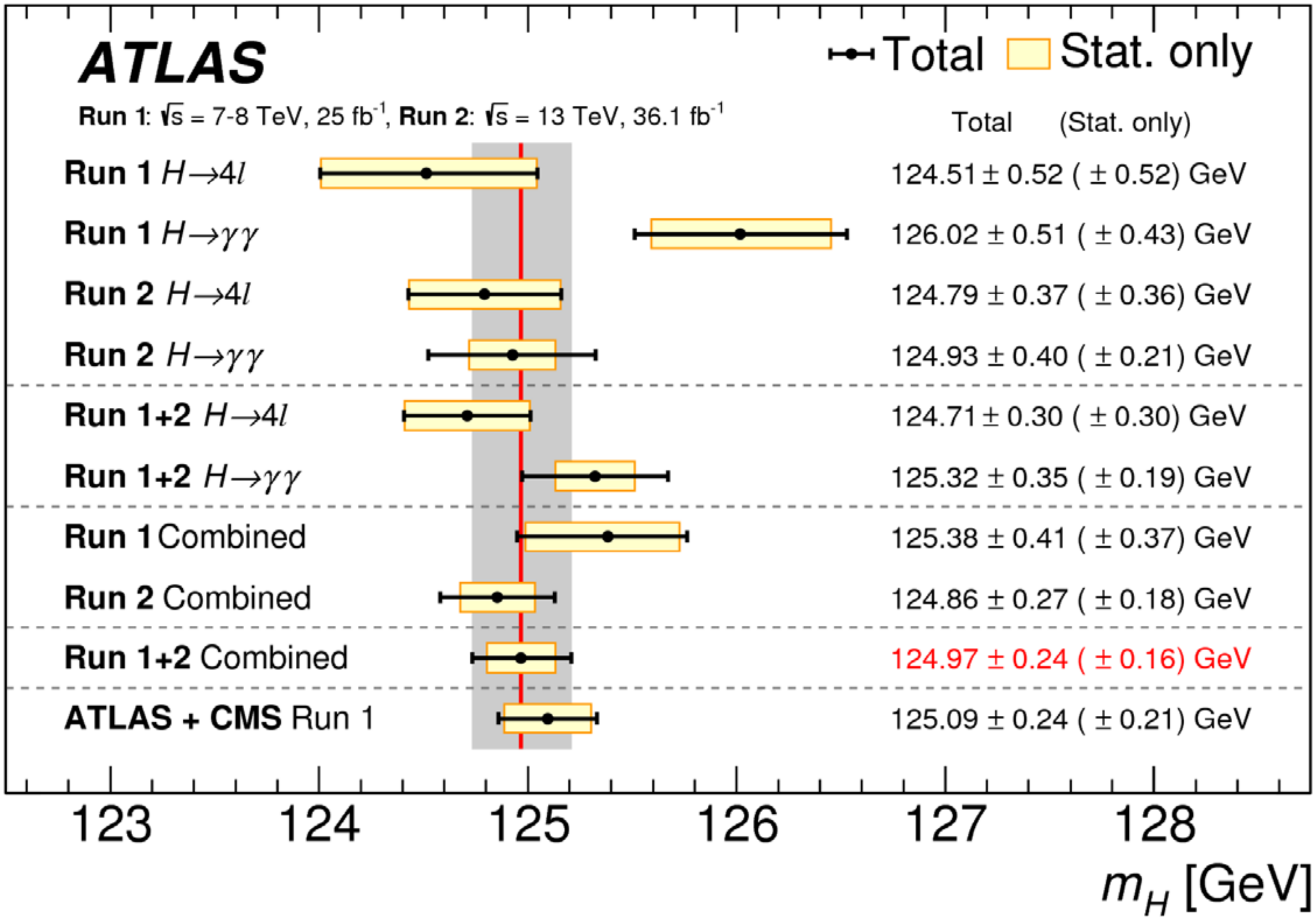

ATLAS
Total
Stat. only
Run 1: √s = 7-8 TeV, 25 fb⁻¹, Run 2: √s = 13 TeV, 36.1 fb⁻¹
Total (Stat. only)
Run 1 H→4l
124.51 ± 0.52 (± 0.52) GeV
Run 1 H→γγ
126.02 ± 0.51 (± 0.43) GeV
Run 2 H→4l
124.79 ± 0.37 (± 0.36) GeV
Run 2 H→γγ
124.93 ± 0.40 (± 0.21) GeV
Run 1+2 H→4l
124.71 ± 0.30 (± 0.30) GeV
Run 1+2 H→γγ
125.32 ± 0.35 (± 0.19) GeV
Run 1 Combined
125.38 ± 0.41 (± 0.37) GeV
Run 2 Combined
124.86 ± 0.27 (± 0.18) GeV
Run 1+2 Combined
124.97 ± 0.24 (± 0.16) GeV
ATLAS + CMS Run 1
125.09 ± 0.24 (± 0.21) GeV
123
124
125
126
127
128
m_H [GeV]

Total width (off-shell measurement)

Constraints on off-shell Higgs boson production and the Higgs boson total width in $ZZ \to 4\ell$ and $ZZ \to 2\ell 2\nu$ final states with the ATLAS detector

The ATLAS Collaboration

A measurement of off-shell Higgs boson production in the $ZZ \to 4\ell$ and $ZZ \to 2\ell 2\nu$ decay channels, where ℓ stands for either an electron or a muon, is performed using data from proton–proton collisions at a centre-of-mass energy of $\sqrt{s} = 13$ TeV. The data were collected by the ATLAS experiment in 2015 and 2016 at the Large Hadron Collider, and they correspond to an integrated luminosity of 36.1 fb^{-1}. An observed (expected) upper limit on the off-shell Higgs signal strength, defined as the event yield normalised to the Standard Model prediction, of 3.8 (3.4) is obtained at 95% confidence level (CL). Assuming the ratio of the Higgs boson couplings to the Standard Model predictions is independent of the momentum transfer of the Higgs production mechanism considered in the analysis, a combination with the on-shell signal-strength measurements yields an observed (expected) 95% CL upper limit on the Higgs boson total width of 14.4 (15.2) MeV.

$\Gamma_{SM} \approx 4.1$ MeV

1904.05105

Higgs → invisible

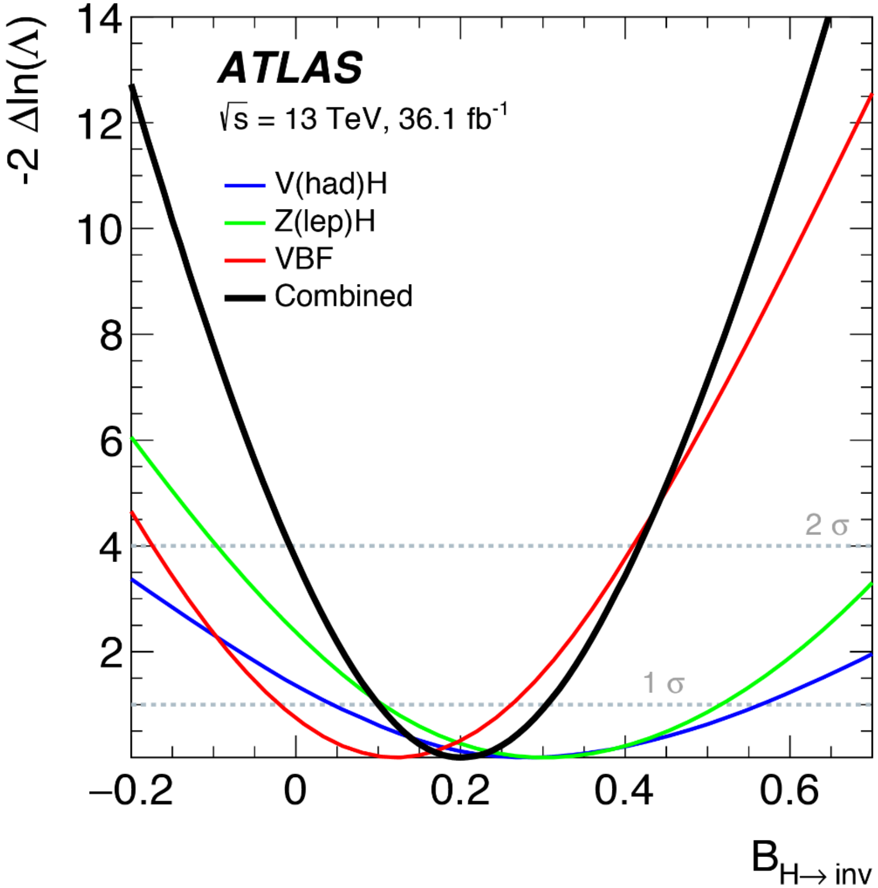

BR < 0.26

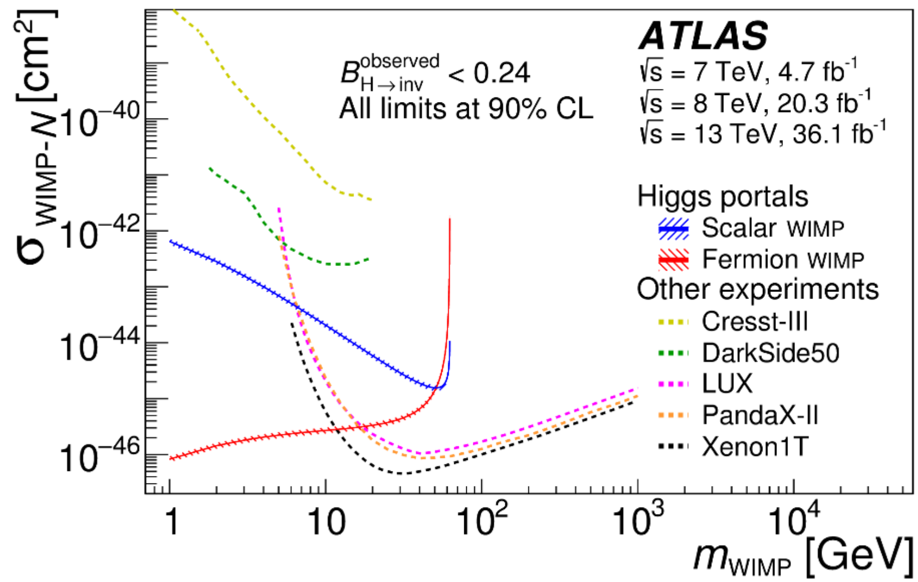

Interpretation in plane of direct detection cross-section vs WIMP mass

H→ quarkonium + γ

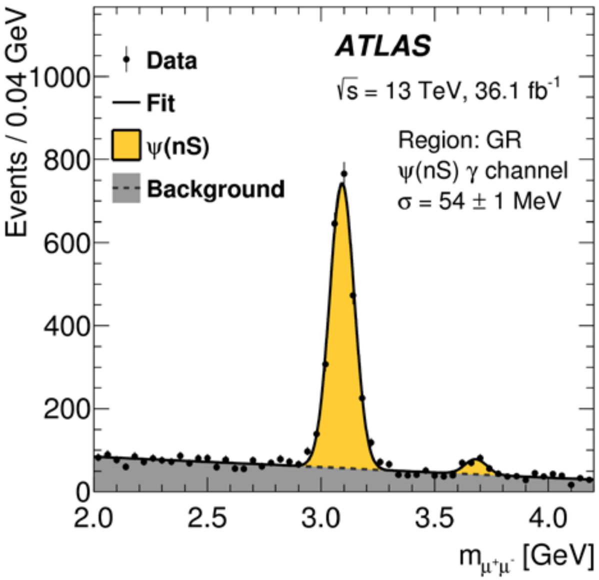

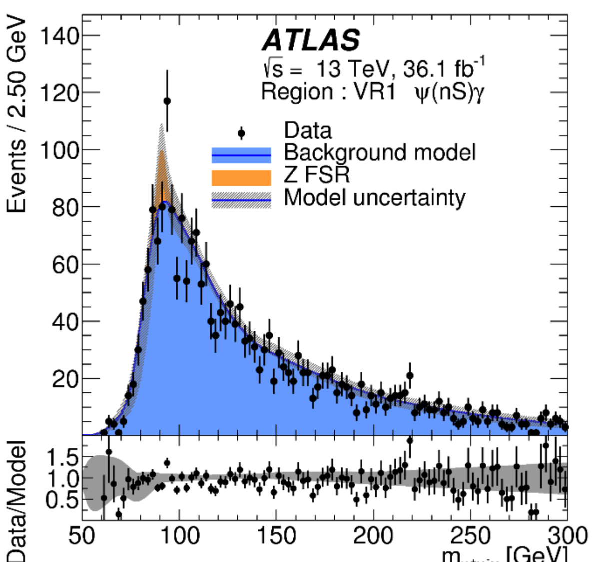

Branching fraction limit (95% CL)	Expected	Observed
$\mathcal{B}(H \to J/\psi\,\gamma)\,[\,10^{-4}\,]$	$3.0^{+1.4}_{-0.8}$	3.5
$\mathcal{B}(H \to \psi\,(2S)\,\gamma)\,[\,10^{-4}\,]$	$15.6^{+7.7}_{-4.4}$	19.8
$\mathcal{B}(Z \to J/\psi\,\gamma)\,[\,10^{-6}\,]$	$1.1^{+0.5}_{-0.3}$	2.3
$\mathcal{B}(Z \to \psi\,(2S)\,\gamma)\,[\,10^{-6}\,]$	$6.0^{+2.7}_{-1.7}$	4.5
$\mathcal{B}(H \to \Upsilon(1S)\,\gamma)\,[\,10^{-4}\,]$	$5.0^{+2.4}_{-1.4}$	4.9
$\mathcal{B}(H \to \Upsilon(2S)\,\gamma)\,[\,10^{-4}\,]$	$6.2^{+3.0}_{-1.7}$	5.9
$\mathcal{B}(H \to \Upsilon(3S)\,\gamma)\,[\,10^{-4}\,]$	$5.0^{+2.5}_{-1.4}$	5.7
$\mathcal{B}(Z \to \Upsilon(1S)\,\gamma)\,[\,10^{-6}\,]$	$2.8^{+1.2}_{-0.8}$	2.8
$\mathcal{B}(Z \to \Upsilon(2S)\,\gamma)\,[\,10^{-6}\,]$	$3.8^{+1.6}_{-1.1}$	1.7
$\mathcal{B}(Z \to \Upsilon(3S)\,\gamma)\,[\,10^{-6}\,]$	$3.0^{+1.3}_{-0.8}$	4.8

The Standard Model Higgs boson decays $H \to J/\psi\,\gamma$ and $H \to \psi(2S)\,\gamma$ offer an opportunity to access the c-quark Yukawa coupling [15, 16] in a manner complementary to studies of the inclusive decay $H \to c\bar{c}$. The branching fraction for $H \to J/\psi\,\gamma$ has been calculated within the SM to be $\mathcal{B}(H \to J/\psi\,\gamma) = (2.99^{+0.16}_{-0.15}) \times 10^{-6}$ [17]. Other recent results on these calculations are given in Refs. [18–20]. For $H \to \psi(2S)\,\gamma$ the branching fraction was calculated by the authors of Ref. [17] to be $\mathcal{B}(H \to \psi(2S)\,\gamma) = (1.03 \pm 0.06) \times 10^{-6}$ using an estimate for the value of the order-v^2 NRQCD long-distance matrix element.

The corresponding decays in the bottomonium sector, $H \to \Upsilon(1S, 2S, 3S)\,\gamma$, can provide, in combination with $H \to b\bar{b}$ decays, information about the real and imaginary parts of the b-quark coupling to the Higgs boson [19], which could probe potential CP violation in the Higgs sector. However, the expected SM branching fractions, $\mathcal{B}(H \to \Upsilon(nS)\,\gamma) = (5.22^{+2.02}_{-1.70}, 1.42^{+0.72}_{-0.57}, 0.91^{+0.48}_{-0.38}) \times 10^{-9}$ $(n = 1, 2, 3)$ [17, 18], are smaller due to a cancellation between the "direct" and "indirect" amplitudes. The direct amplitude proceeds through the $H \to q\bar{q}$ coupling with a subsequent photon emission before the $q\bar{q}$ hadronisation to $\Upsilon(nS)$. The indirect amplitude proceeds via the $H\gamma\gamma$ coupling followed by the fragmentation $\gamma^* \to \Upsilon(nS)$.

Indirect constraint on charm Yukawa

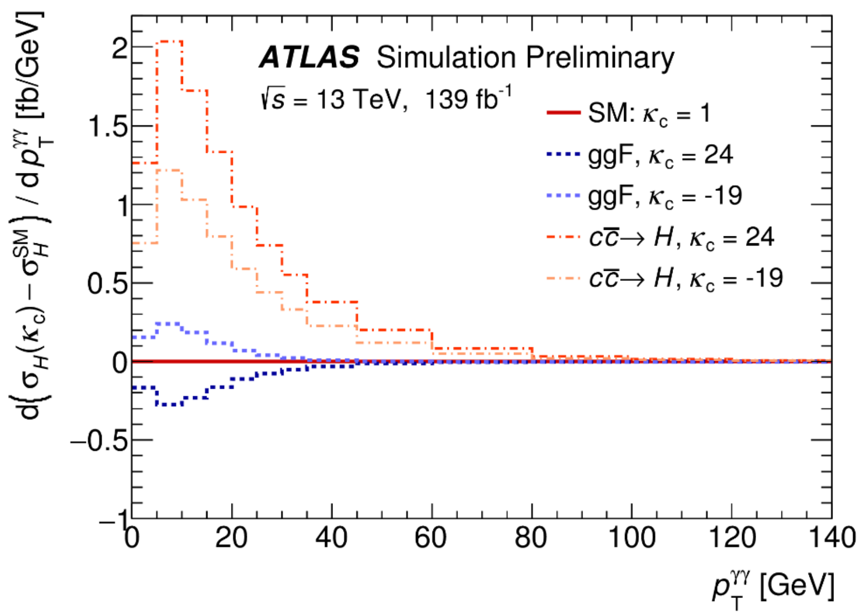

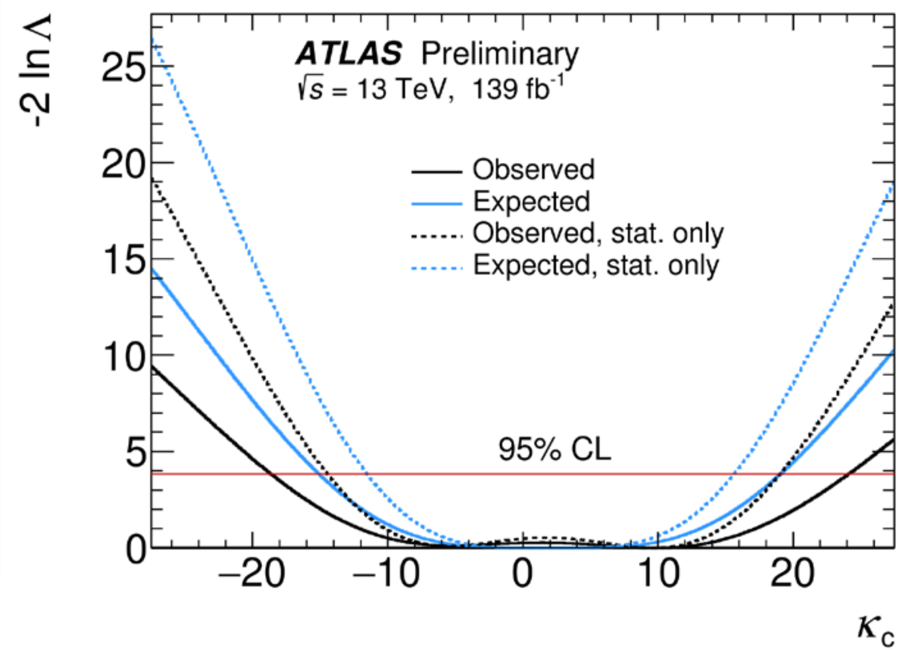

cc → H affects H p_T distribution

Coefficient	Observed 95% CL limit	Expected 95% CL limit
κ_c	$[-19, 24]$	$[-15, 19]$

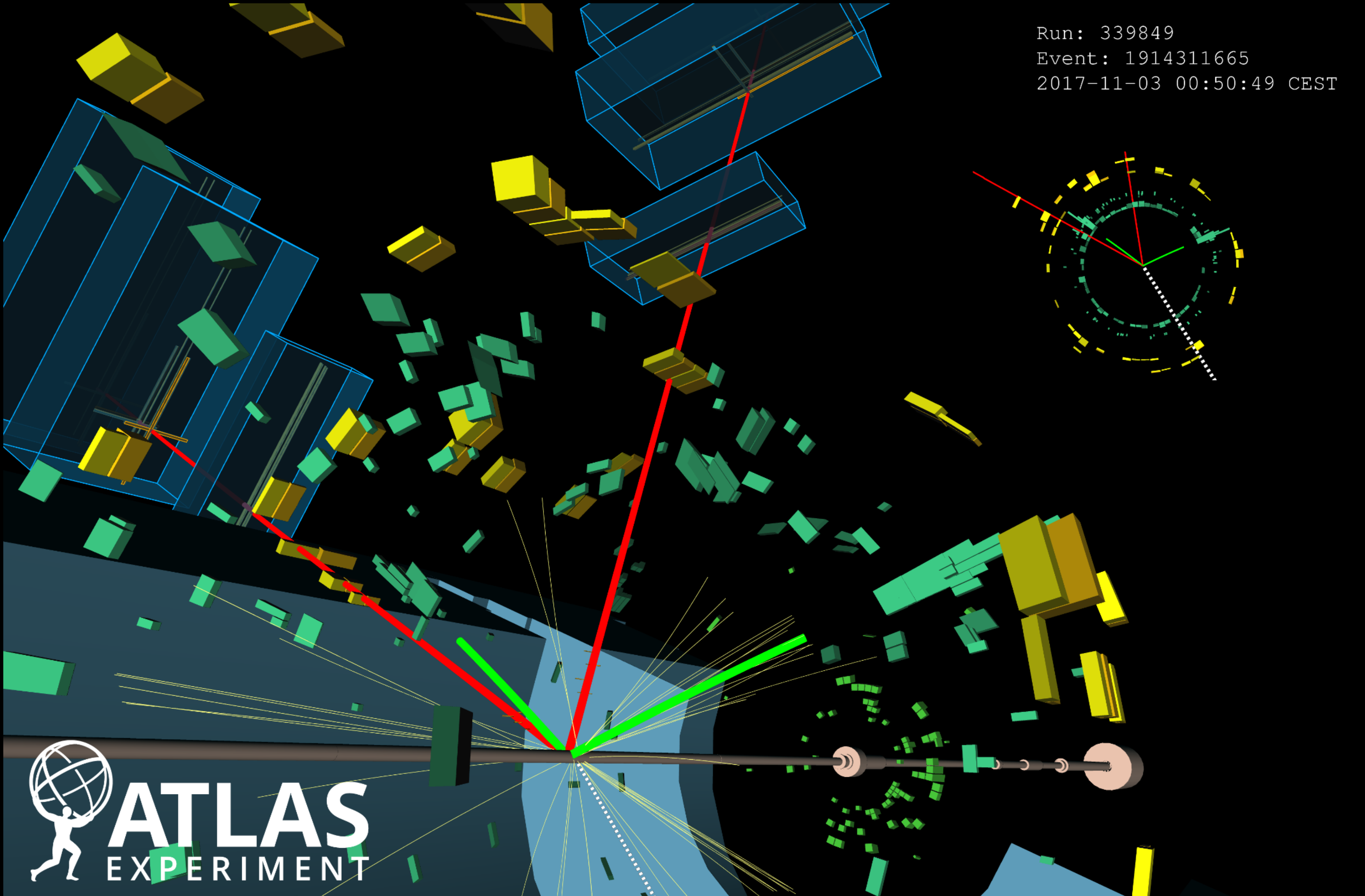

VH: H → eeμμ candidate

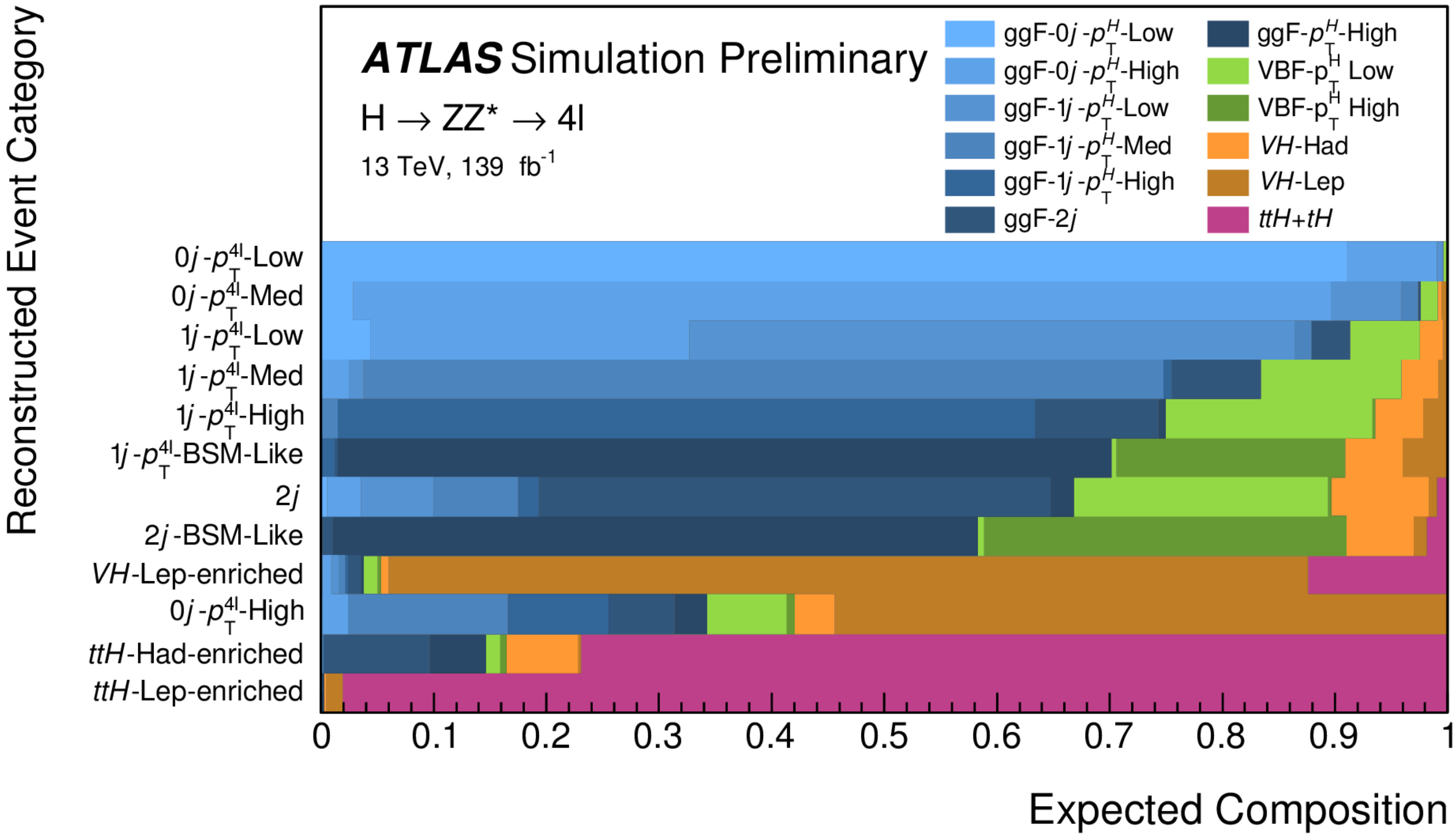
ATLAS Simulation Preliminary
H → ZZ* → 4l
13 TeV, 139 fb-1
ggF-0j-pT^H-Low
ggF-0j-pT^H-High
ggF-1j-pT^H-Low
ggF-1j-pT^H-Med
ggF-1j-pT^H-High
ggF-2j
ggF-pT^H-High
VBF-pT^H Low
VBF-pT^H High
VH-Had
VH-Lep
ttH+tH
Reconstructed Event Category
0j-pT^4l-Low
0j-pT^4l-Med
1j-pT^4l-Low
1j-pT^4l-Med
1j-pT^4l-High
1j-pT^4l-BSM-Like
2j
2j-BSM-Like
VH-Lep-enriched
0j-pT^4l-High
ttH-Had-enriched
ttH-Lep-enriched
0
0.1
0.2
0.3
0.4
0.5
0.6
0.7
0.8
0.9
1
Expected Composition

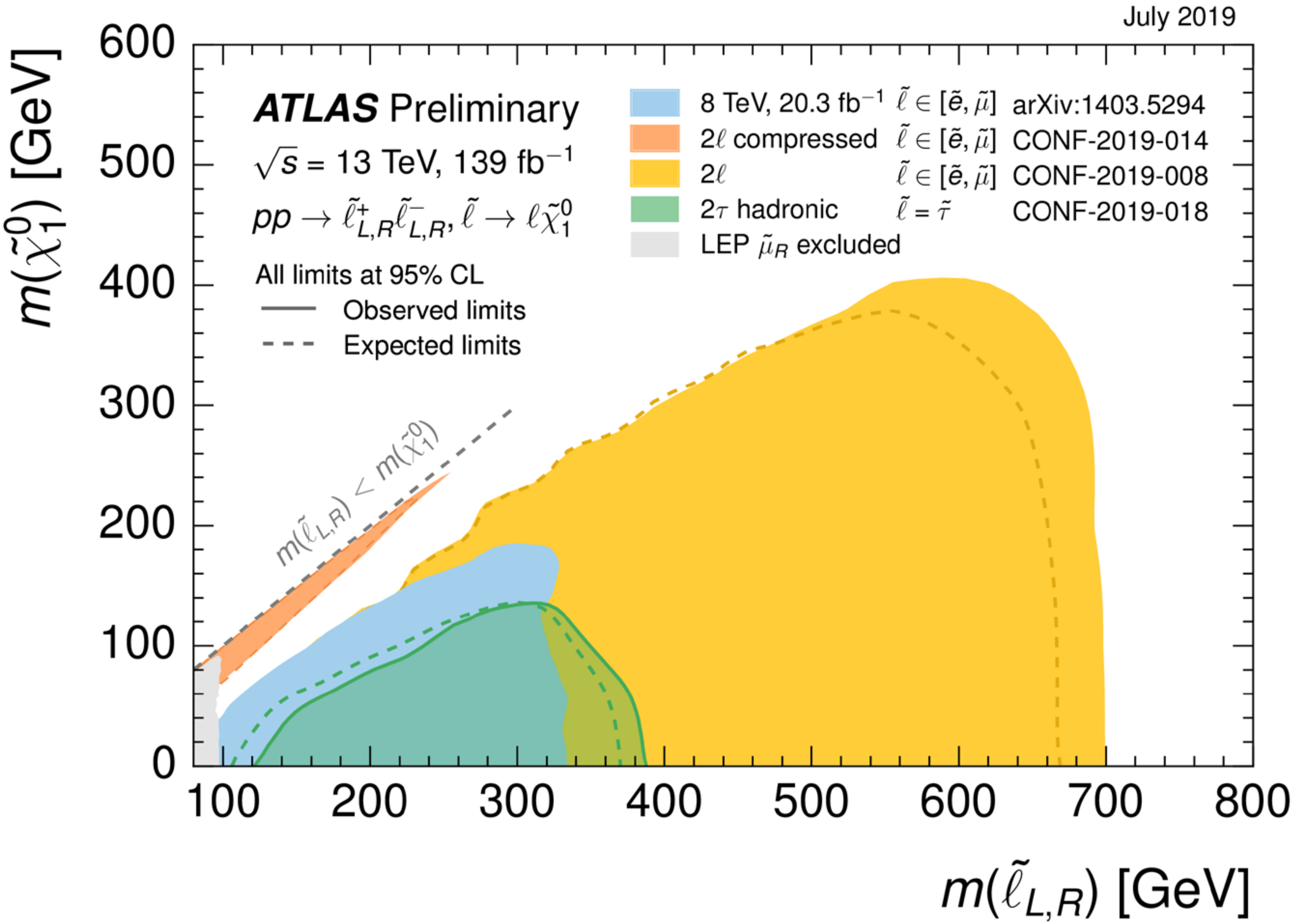
July 2019
ATLAS Preliminary
$\sqrt{s}$ = 13 TeV, 139 fb^{-1}
$pp \to \tilde{\ell}^+_{L,R}\tilde{\ell}^-_{L,R}, \tilde{\ell} \to \ell\tilde{\chi}^0_1$
All limits at 95% CL
Observed limits
Expected limits
8 TeV, 20.3 fb^{-1} $\tilde{\ell} \in [\tilde{e}, \tilde{\mu}]$ arXiv:1403.5294
2ℓ compressed $\tilde{\ell} \in [\tilde{e}, \tilde{\mu}]$ CONF-2019-014
2ℓ $\tilde{\ell} \in [\tilde{e}, \tilde{\mu}]$ CONF-2019-008
2τ hadronic $\tilde{\ell} = \tilde{\tau}$ CONF-2019-018
LEP $\tilde{\mu}_R$ excluded
$m(\tilde{\ell}_{L,R}) < m(\tilde{\chi}^0_1)$
$m(\tilde{\chi}^0_1)$ [GeV]
$m(\tilde{\ell}_{L,R})$ [GeV]
0
100
200
300
400
500
600
700
800

ATLAS-CONF-2019-029

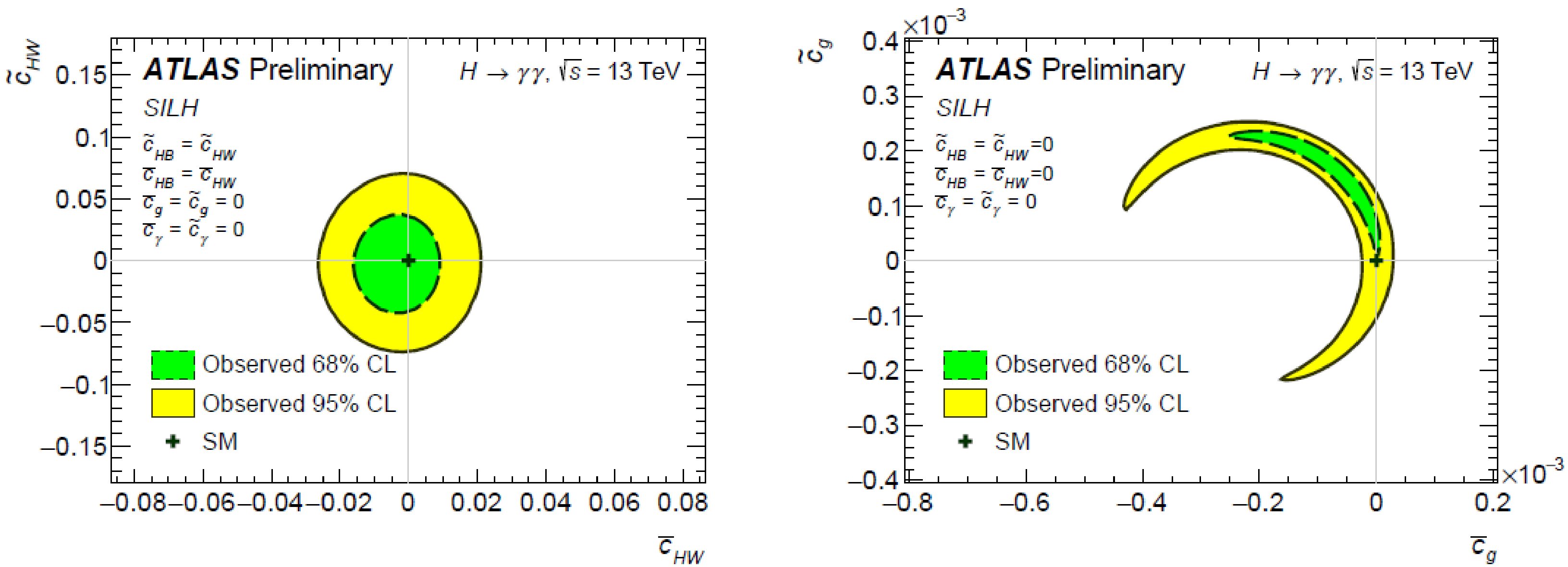

(a) (b)

Figure 12: The observed 68% (green) and 95% (yellow) confidence level regions from the simultaneous fit to the $\bar{c}_{HW}$ and $\tilde{c}_{HW}$ Wilson coefficients of the SILH basis are shown in the left plot (a). The values of $\bar{c}_{HB}$ and $\tilde{c}_{HB}$ are set to be equal to $\bar{c}_{HW}$ and $\tilde{c}_{HW}$, respectively, and all other Wilson coefficients are set to zero. The SM expectation at (0, 0) is also shown. The corresponding limits from the simultaneous fit to $\bar{c}_g$ and $\tilde{c}_g$, setting all other Wilson coefficients to zero, are shown in the right plot (b).

Constraints on a different EFT basis (SILH) on two parameters

Search for diboson resonances in hadronic final states in 139 fb^{-1} of pp collisions at $\sqrt{s}$ = 13 TeV with the ATLAS detector

The ATLAS Collaboration

Narrow resonances decaying into WW, WZ or ZZ boson pairs are searched for in 139 fb^{-1} of proton–proton collision data at a centre-of-mass energy of $\sqrt{s}$ = 13 TeV recorded with the ATLAS detector at the Large Hadron Collider from 2015 to 2018. The diboson system is reconstructed using pairs of high transverse momentum, large-radius jets. These jets are built from a combination of calorimeter- and tracker-inputs compatible with the hadronic decay of a boosted W or Z boson, using jet mass and substructure properties. The search is performed for diboson resonances with masses greater than 1.3 TeV. No significant deviations from the background expectations are observed. Exclusion limits at the 95% confidence level are set on the production cross-section times branching ratio into dibosons for resonances in a range of theories beyond the Standard Model, with the highest excluded mass of a new gauge boson at 3.8 TeV in the context of mass-degenerate resonances that couple predominantly to gauge bosons.

bϕ, ϕ→bb

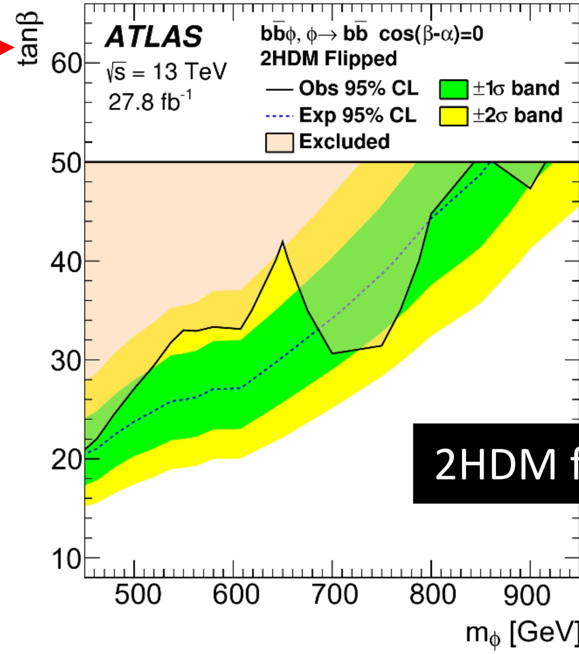

2HDM flipped

tan(β) enhancement of b-quark couplings (but not τ leptons)

Table 1: Tree-level fermion couplings of the 2HDM h, H, and A bosons for model types I, II, X (or lepton-specific), and Y (or flipped). Here U, D, and E refer to up-type quarks, down-type quarks, and charged leptons, respectively, $t_\beta \equiv \tan\beta$ is the ratio of the vacuum expectation values of the two scalar doublets, and $\epsilon = \cos(\beta - \alpha)$ where α is the mixing angle of the two CP-even scalar bosons [9]. The couplings are normalized to the SM Higgs boson couplings $h_{\text{SM}}\bar{U}U$, $h_{\text{SM}}\bar{D}D$, and $h_{\text{SM}}\bar{E}E$ and are given in the alignment limit $\cos(\beta - \alpha) \approx 0$ where the couplings of the light scalar boson h are close to SM expectations.

	$h\bar{U}U$	$h\bar{D}D$	$h\bar{E}E$	$H\bar{U}U$	$H\bar{D}D$	$H\bar{E}E$	$iA\bar{U}\gamma_5 U$	$iA\bar{D}\gamma_5 D$	$iA\bar{E}\gamma_5 E$
I	$1+\frac{\epsilon}{t_\beta}$	$1+\frac{\epsilon}{t_\beta}$	$1+\frac{\epsilon}{t_\beta}$	$-(\frac{1}{t_\beta}-\epsilon)$	$-(\frac{1}{t_\beta}-\epsilon)$	$-(\frac{1}{t_\beta}-\epsilon)$	$-\frac{1}{t_\beta}$	$\frac{1}{t_\beta}$	$\frac{1}{t_\beta}$
II	$1+\frac{\epsilon}{t_\beta}$	$1-\epsilon t_\beta$	$1-\epsilon t_\beta$	$-(\frac{1}{t_\beta}-\epsilon)$	$t_\beta+\epsilon$	$t_\beta+\epsilon$	$-\frac{1}{t_\beta}$	$-t_\beta$	$-t_\beta$
X	$1+\frac{\epsilon}{t_\beta}$	$1+\frac{\epsilon}{t_\beta}$	$1-\epsilon t_\beta$	$-(\frac{1}{t_\beta}-\epsilon)$	$-(\frac{1}{t_\beta}-\epsilon)$	$t_\beta+\epsilon$	$-\frac{1}{t_\beta}$	$\frac{1}{t_\beta}$	$-t_\beta$
Y	$1+\frac{\epsilon}{t_\beta}$	$1-\epsilon t_\beta$	$1+\frac{\epsilon}{t_\beta}$	$-(\frac{1}{t_\beta}-\epsilon)$	$t_\beta+\epsilon$	$-(\frac{1}{t_\beta}-\epsilon)$	$-\frac{1}{t_\beta}$	$-t_\beta$	$\frac{1}{t_\beta}$